Fast Inertial Relaxation Engine in the CRYSTAL Code

Chiara Ribaldone[1, a)] and Silvia Casassa[1]
Department of Theoretical Chemistry, University of Turin, Turin, Italy

(Dated: 31 December 2021)

In the framework of *ab initio* simulations, the search for energy minimum atomic structures is the first step to perform in studying the properties of a system. One of the most used and efficient optimization algorithm is a quasi-Newton line-search scheme based on Broyden-Fletcher-Goldfarb-Shanno (Bfgs) Hessian updating formula. However, recent studies [E. Bitzek et al., Phys. Rev. Lett. 97, 170201 (2006) and J. Guénolé et al., Comput. Mater. Sci. 175, 109584 (2020)] suggested that minimization methods based on Molecular Dynamics concepts, such as the Fast Relaxation Inertial Engine (Fire) algorithm, often exhibit better performance and accuracy in finding local minima than line-search based schemes. In the present work, the implementation of Fire, in the framework of Crystal *ab initio* quantum mechanical simulation package, [R. Dovesi et al., Wiley Interdiscip. Rev. Comput. Mol. Sci. 8, e1360 (2018)] has been described. Its efficiency and performance in comparison with Bfgs quasi-Newton scheme has been assessed, using Hartree-Fock and Density Functional Theory with Perdew-Burke-Ernzerhof and hybrid functionals to model the potential energy surface. Fire shows good convergence behavior for all the considered systems, well reproducing the minimum energy structures obtained by Bfgs approach. As regards the computational cost, Fire requires more iterations to converge with respect to Bfgs, but each Fire iteration is faster than the Bfgs one. The overall efficiency of Fire improves as the size of the system increased, so that this minimization method seems very promising for systems without symmetry (space group P_1) with a large number of atoms.

I. INTRODUCTION

Structural optimization of molecular and crystalline systems becomes an increasingly more common task in solid state physics, chemistry, biology and materials science. In fact, it is the obligatory starting point for the calculation of any of the ground state properties of a system, such as electronic, mechanical, optical and transport properties. The optimized structure corresponds to a local minimum energy configuration in the Potential Energy Surface (Pes) and, as the size and complexity of the systems rise up, the modeling of such multidimensional shape and the search of its critical points becomes more and more challenging. As a matter of fact, a variety of well-established multidimensional minimization methods are adopted to find optimized configurations, among which the quasi-Newton algorithm[1,2] in conjunction with the efficient Broyden-Fletcher-Goldfarb-Shanno (Bfgs) updating scheme for the Hessian matrix,[3–7] is heralded as a benchmark method.

The Crystal code,[8] an *ab initio* computational package for the study of molecular and crystalline systems, based on Hartree Fock (Hf) method and Density Functional Theory (Dft), performs structural optimizations through a quasi-Newton procedure, in which the default choice for the initial Hessian matrix is obtained from a model Hessian, as proposed by Schlegel,[9,10] and its update is performed by using the Schlegel's (Sh) scheme[11] or the efficient Broyden-Fletcher-Goldfarb-Shanno (Bfgs) algorithm.[3–7]

This method has proved to be effective in a wide range of different applications. Nevertheless, it is worth to note that (i) the potential energy surface is locally described with a function expanded up to its second order derivative (i.e. the Pes is approximated to be of quadratic form) and (ii) the calculation of the approximated Hessian matrix requires a computational cost which scales approximately linearly with the system size. At the same time, the recent development of a molecular dynamics module[12] in the Crystal code paved the way for an exploration of methods based on Md techniques, such as the search for transition states and global minimization algorithms. The interest in these methods is driven by the purpose of testing the Md module reliability and efficiency, extending its capabilities in order to provide the Users a robust and complete Md package. In this context, with the aim to complement Crystal's abilities and overcome some of its limitations, we turned our attention to a novel approach recently proposed by E. Bitzek et al.,[13] called the Fast Inertial Relaxation Engine (Fire). This simple and robust algorithm is based on molecular dynamics (Md) concepts and seems to be promising both in its basic[13] and improved[14] implementation. It has been demonstrated to be a useful tool in numerous atomistic studies, including Dft based simulations of chemically complex systems,[15–18] significantly faster than standard implementation of the Conjugate Gradient (Cg) algorithm and often competitive with more sophisticated quasi-Newton schemes as typified by the Bfgs method.[13,19] Moreover, it seems very well suited for transition state calculations in conjunction with the Nudged Elastic Band method,[20] and apparently it works efficiently in the case of noisy potential energy surface, where Bfgs minimization often fails.[21]

Furthermore, the Fire scheme (i) does not require

a)chiara.ribaldone@unito.it

any approximation of the shape of the potential energy surface, possibly resulting in better performances for systems which are far from the equilibrium and (ii) does not involve the approximation of the Hessian matrix, conceivably leading to a reduction of the computational cost as the size of the system increases.
On the heels of these results, FIRE algorithm has been implemented in several atomistic simulation packages, like LAMMPS,[22] GROMACS,[23] IMD,[24] DL_POLY,[25] EON,[26] or ASE.[27]
In the present work, the implementation of the FIRE algorithm in the CRYSTAL code is described and its efficiency, in terms of accuracy and timing, is assessed. The results obtained with the basic and improved version of FIRE are compared with the quasi-Newton minimization methods based on SH and BFGS updating schemes. The effect of the exchange and correlation functional, which determines the shape of the PES, is explored, adopting different Hamiltonian forms such as HF, pure DFT and hybrids. Different kind of systems are considered, covering various dimensionalities and the whole range of chemical interactions, with the aim of investigating the portability of the method, its advantages and limitations.
The article is structured as follows. In Section II the FIRE algorithm and its implementation in the CRYSTAL code is outlined. Then, in Section III, the meaning and tuning of FIRE specific parameters is discussed, some default values are suggested and a general strategy for their optimization is proposed. In Section IV, the results of the structural minimizations performed with FIRE are shown and compared with those obtained with the SH and BFGS schemes. Finally, in Section VI, the general computational details used to perform the calculations are provided.

II. THE FIRE ALGORITHM

In a system with N nuclei of mass m, whose positions is associated to the coordinates $\boldsymbol{x} = (x_1, x_2, ..., x_{3N})$, the potential energy surface described by $E(\boldsymbol{x})$ is a map $E : \mathbb{R}^{3N} \rightarrow \mathbb{R}$ that assigns to each atomic configuration $\boldsymbol{x}$ a potential energy value $E(\boldsymbol{x})$.
FIRE algorithm is based on the equation of motion for the nuclei as proposed by E. Bitzek et al.,[13] that determines the motion of the system in the potential energy surface by introducing a corrected acceleration

$$\dot{\boldsymbol{v}}(t) = \frac{\mathbf{F}(\boldsymbol{x}(t))}{m} - \gamma(t)\,\|\boldsymbol{v}(t)\|\,[\hat{\boldsymbol{v}}(t) - \hat{\mathbf{F}}(\boldsymbol{x}(t))] \quad (1)$$

where hat indicates unit vectors, $\|\boldsymbol{v}(t)\|$ is the euclidean norm of the $3N$ velocity vector and $\gamma(t)$ is a scalar function of time. The first term on the right hand side in Eq. (1) represents regular classical Newtonian dynamics. The effect of the second term is to direct the trajectory towards the steepest descent at $\boldsymbol{x}(t)$ by reducing the angle between $\boldsymbol{v}(t)$ and $\mathbf{F}(\boldsymbol{x}(t))$.
The explicit-Euler discretization of the equation of motion in Eq. (1), with initial condition $\boldsymbol{v}(t=0) = \mathbf{0}$, leads to the following velocities updating expression

$$\begin{aligned}
&\boldsymbol{v}(t+dt) = \boldsymbol{v}(t) + \dot{\boldsymbol{v}}(t)dt \\
&= \boldsymbol{v}(t) + \left\{ \frac{\mathbf{F}(\boldsymbol{x}(t))}{m} - \gamma(t)[\boldsymbol{v}(t) - \|\boldsymbol{v}(t)\|\,\hat{\mathbf{F}}(\boldsymbol{x}(t))] \right\} dt \\
&= (1-\alpha)\boldsymbol{v}(t) + \alpha\|\boldsymbol{v}(t)\|\,\hat{\mathbf{F}}(\boldsymbol{x}(t)) + \frac{\mathbf{F}(\boldsymbol{x}(t))}{m} dt \\
&= \tilde{\boldsymbol{v}}(t) + \frac{\mathbf{F}(\boldsymbol{x}(t))}{m} dt \qquad (2)
\end{aligned}$$

with $\alpha = \gamma(t)\,dt$ and

$$\tilde{\boldsymbol{v}}(t) = (1-\alpha)\boldsymbol{v}(t) + \alpha\|\boldsymbol{v}(t)\|\,\hat{\mathbf{F}}(\boldsymbol{x}(t)) \qquad (3)$$

Eq. (2) can be thus interpreted as the classical Newton equation in which the velocity $\boldsymbol{v}(t)$ of each atom at the time t has been replaced by the modified velocity $\tilde{\boldsymbol{v}}(t)$. Then, after the redefinition of $\boldsymbol{v}(t)$ through Eq. (2), a conventional molecular dynamics integrator, as the one recently implemented in the CRYSTAL code,[12] can be used to compute the velocities $\boldsymbol{v}(t+dt)$ at time $(t+dt)$.
In the CRYSTAL code, the forces acting on the nuclei, $\mathbf{F}(\boldsymbol{x}(t)) = -\nabla E(\boldsymbol{x}(t))$, are computed analytically through the Hellmann-Feynman theorem,[28] so that the energy $E(\boldsymbol{x}(t))$ involved corresponds to the electronic ground state total energy of the system for a particular nuclear configuration.
A global quantity called power factor, $P(t)$, defined as

$$P(t) = \sum_{i=1}^{3N} F_i(\boldsymbol{x}(t)) \cdot v_i(t) = \mathbf{F}(\boldsymbol{x}(t)) \cdot \boldsymbol{v}(t) \qquad (4)$$

is used to monitor and direct the optimization process. $P(t)$ corresponds to the power being delivered to the nuclei by the force acting on them. Since the total force acting on the system and the total energy gradient have opposite directions, if the global velocity of the system points in a direction of higher energy, the scalar product between the force and the velocity, i.e. $P(t)$, is negative. So, the motion of the system in the PES is forced to change according to the sign of $P(t)$, with both the timestep dt and the mixing factor α treated as dynamically adaptive quantities. If $P(t) > 0$, the α mixing parameter is decreased by a factor α_{dec} and the timestep is increased by a factor dt_{inc}, with an upper bound equal to the largest possible timestep dt_{max}. As a consequence, the system is accelerated in the direction of the energy minimum. Otherwise, when $P(t) \leq 0$, the algorithm reacts as follows: (i) the system is immediately frozen by setting all the velocities to zero ($\boldsymbol{v} = \mathbf{0}$) to avoid uphill motions, (ii) the timestep is reduced by a factor dt_{dec} to ensure a smooth restart, (iii) the α parameter is reset to its initial value α_{in} and (iv) to ensure better stability, a short latency time of N_{del} steps can be imposed before accelerating the dynamics again.
As a side note, it should be underlined that the FIRE minimization optimizes only the nuclei positions, letting the volume and the lattice parameters unchanged.

A. The FIRE2.0 algorithm

The FIRE2.0 scheme is an improvement of the previously described basic version of the algorithm, by introducing five main variations to the FIRE procedure as listed below.[14]

(a) In order to correct uphill motion when $P(t) \leq 0$ is detected, the trajectory of the atomic system on the PES is moved backward by half a timestep by means of the formula

$$\boldsymbol{x}(t) \;\rightarrow\; \boldsymbol{x}(t) - \frac{dt}{2}\boldsymbol{v}(t) \tag{5}$$

(b) The mixing of the velocity and force vectors described by Eq. (3) is performed just after the velocities updating by half a timestep $\boldsymbol{v}(t+0.5\,dt)$ in the Velocity Verlet algorithm, instead of before the integration of the equations of motions through the Velocity Verlet scheme.

(c) The minimization is stopped if the number of consecutive iterations with $P(t) \leq 0$ exceeds a threshold given by $N_{ple,max}$. This additional stopping criterion has the aim to avoid unnecessary looping, when further minimization of the geometry of the system does not appear to be feasible. This is the case for regions of the PES which can be described as narrow valleys, where the system could eventually be trapped without finding a different minimum.

(d) A minimum value for the timestep is defined, so that the timestep used for the integration can not be decreased below an established value dt_{min}.

(e) In the case of $P(t) \leq 0$ and if the minimum timestep is not yet reached, the timestep is decreased only when the number of FIRE iterations is greater than N_{del}, i.e., if $P(t) \leq 0$ the decrease of the timestep is performed only after N_{del} optimization steps.

In particular, modifications (a) and (b) are supposed to introduce the major discrepancies and differences in FIRE2.0 minimization with respect to the basic FIRE one.

III. FIRE IN CRYSTAL CODE

A. Molecular Dynamics integrator

As highlighted by F. Shuang et al.,[19] the MD integrator chosen to update positions and velocities at each iteration has a relevant influence on the performance of FIRE minimization procedure. In particular, the Velocity Verlet integrator has been demonstrated to be an optimal choice along with FIRE optimization, showing good efficiency and convergence.[19] Thanks to its robust behavior, the Velocity Verlet integrator has been adopted as default molecular dynamics integrator in the implementation of FIRE algorithm. For the case of FIRE2.0 scheme, a slightly modified Velocity Verlet procedure is implemented, where the velocities updating by means forces and velocity mixing given by Eq. (3) is embedded in the MD integrator, as explained in point (b) of Section II A.

B. Convergence criteria

Four kind of convergence criteria are implemented in the CRYSTAL code for FIRE structural minimization, respectively based on (i) the normalized euclidean norm (i.e. the root mean square) of nuclear forces vector, given by

$$F_{rms} = \frac{1}{\sqrt{3N}}\left[\sum_{i=1}^{N}(F_{x,i}^2 + F_{y,i}^2 + F_{z,i}^2)\right]^{1/2} \tag{6}$$

and computed in cartesian coordinates, (ii) the difference in energy between two consecutive optimization steps, (iii) the maximum and (iv) root-mean-square displacement of the atomic positions between the n-th step and the previous $(n-1)$-th one, both computed in cartesian coordinates. By default, when these four conditions are all satisfied at a time, FIRE optimization is considered complete. However, it is also possible for the Users to adopt only one of these convergence criteria, and to modify the default values of the thresholds, using specific Input keywords.
Nevertheless, the normalized euclidean norm of cartesian nuclear forces, computed as in Eq. (6), has proven to be a reliable and sufficiently strict check to assess the degree of relaxation in FIRE and FIRE2.0,[14] and is therefore used in this work as the *only* convergence criterion.

C. Setting of Fire default parameters

The adjustable parameters in FIRE algorithm are (i) the initial value α_{in} of the mixing parameter to be used in Eq. (2), (ii) the initial timestep dt_{in}, (iii) its maximum value $dt_{max} = dt_{in} \cdot t_{max}$, and (iv) N_{del}, i.e. the number of self-consistent cycles (SCF) and force evaluations (GRAD) to be performed, after a stop due to $P(t) \leq 0$, before accelerating the dynamics again.
It is worth to note that a good assessment of the set of parameters, namely (α_{in}, dt_{in}, t_{max}, N_{del}), is essential to fully exploit the efficiency of FIRE optimization scheme, but, within a wide range of variability of these parameters, it does not affect the reliability of the final results. Based on our experience, and with reference to four systems of different dimensionality, i.e. a water molecule, a water polymer, a 2D slab of ice and a urea crystal, modeled through a PBE functional, a 3-steps procedure is proposed to disentangled the effect of the different parameters and adjust their values. In

all cases, the goal is to minimize the number of iterations N_{step} (in each step, a self-consistent cycle (SCF) procedure and an energy gradient calculation (GRAD) are performed), as follows:
(i) for a given dt_{in} and N_{del}, different values of t_{max} are explored (as in Figs. 1a,d and 2a,d) in order to choose its optimal value;
(ii) then, given the best value of t_{max} (and fixing N_{del}), different dt_{in} are evaluated in the range $[0.1, 3.0]$ fs, to define its best value (Figs. 1b,e and 2b,e);
(iii) finally, having fixed the optimal values of t_{max} and dt_{in}, N_{del} can be varied in the range $[0, 10]$, as shown in Figs. 1c,f and 2c,f. The best value for α_{in} is automatically derived from the overall analysis of all the trends obtained.
A very similar behavior of the number of total iterations N_{step} as a functions of the initial mixing factor α_{in} for points (i), (ii) and (iii) is obtained with all the atomic systems considered, suggesting that the best set of FIRE parameters does not depend on the dimensionality of the system. Furthermore, despite the difference in the number of iterations necessary to reach convergence, the reliability of FIRE in finding the minimum energy structure is preserved.
As regards the FIRE2.0 version, the scan of the performance dependency on the input parameters leads to a trend analogous as the one found for the basic FIRE, with a general translation of the observed curves towards low values number of optimization steps N_{step} due to the higher efficiency of FIRE2.0 with respect to the basic implementation. Therefore, the same default input parameters can be used for both FIRE and FIRE2.0 minimizations. As a result of this analysis, it becomes clear that a set of parameters which provides excellent performance and is optimal for a wide range of systems, different in size, dimension and chemical-physical properties, can be defined. Finally, the default values for α_{dec}, dt_{inc} and dt_{dec} factors, used to accelerate or decrease the entity of the atomic motion, and for the parameters t_{min} and $N_{ple,max}$, introduced in the FIRE2.0 algorithm, are taken to be equal to those originally proposed by Bitzek et al.[13,14] These default values, obviously modifiable from Input, are shown in Table I.
It is worth to note that all the FIRE parameters screening is here performed using PBE functional. However, from a preliminary analysis in the case of water molecule and urea crystal with B3LYP functional, the best set of FIRE parameters results slightly dependent on the kind of exchange-correlation functional employed. For the case of water molecule, for instance, the best set of FIRE parameters $(\alpha_{in}, dt_{in}, t_{max}, N_{del})$ with PBE and B3LYP functional is, respectively, $(0.35, 2.0, 1.0, 0)$ and $(0.20, 1.0, 1.0, 0)$, leading to a corresponding total number of optimization steps equal to 26 and 32.

TABLE I: CRYSTAL default values for FIRE algorithm parameters, with the correspondent keywords that can be used in Input to modify their values. The last two parameters are defined only for FIRE2.0 version of the algorithm.

	Parameter	Keyword	Default value	
FIRE	α_{in}	ALPHASTART	0.30	FIRE2.0
	dt_{in}	DTSTART	1.0 (fs)	
	t_{max}	TMAX	1.0	
	N_{del}	NDELAY	0	
	α_{dec}	ALPHASHRINK	0.99	
	dt_{inc}	DTGROW	1.1	
	dt_{dec}	DTSHRINK	0.5	
	$N_{ple,max}$	NPLEZEROMAX	2000	
	t_{min}	TMIN	0.02	

IV. RESULTS AND DISCUSSION

The performance of FIRE algorithm, at constant volume and lattice parameters, has been evaluated for systems with different dimensionality, number of atoms and kind of chemical bond. The geometry optimization on the same set of systems has been also performed with quasi-Newton SH and BFGS updating schemes, removing the symmetry of the systems, if necessary, to allow a reliable comparison with FIRE procedure. Information on each system (geometry structures, basis sets and computational settings) are reported in the Supplementary Material (SM). The number of optimization steps up to convergence, N_{step}, the mean number of self consistent cycle $\bar{N}_w$ performed in the calculation of the ground state solution at each optimization step, the root mean square of final forces, F_{rms}, of last iteration atomic displacements, d^e_{rms}, and of bond lengths difference between SH or FIRE and BFGS, Δb_{rms}, are summarized in Table II. The number of degrees of freedom in FIRE structural optimizations is equal to three times the number of atoms N_{at} in the reference cell unit, while for SH and BFGS equals $(3N_{at} - 6)$ for molecules and $(3N_{at} - 3)$ for periodic systems.
The specific parameters adopted in FIRE for each system are reported in Table 3 of the SM. As regards the general performances, the results show that each single FIRE optimization cycle (which also involves SCF $\oplus$ GRAD calculations) has a less computational cost than the corresponding SH and BFGS one. Indeed, in FIRE minimization the mean number of self-consistent iterations $\bar{N}_w$ employed to reach convergence for the ground state wavefunction calculations at each iteration is less than the correspondent number for the quasi-Newton methods, as reported in Table II. On average, this means that FIRE method displaces the nuclei at each iteration less than SH and BFGS. The less the displacement at each step, the better the wavefunction input guess at the next iteration, the less the number of self-consistent cycles needed for ground-state wavefunction convergence. This inter-

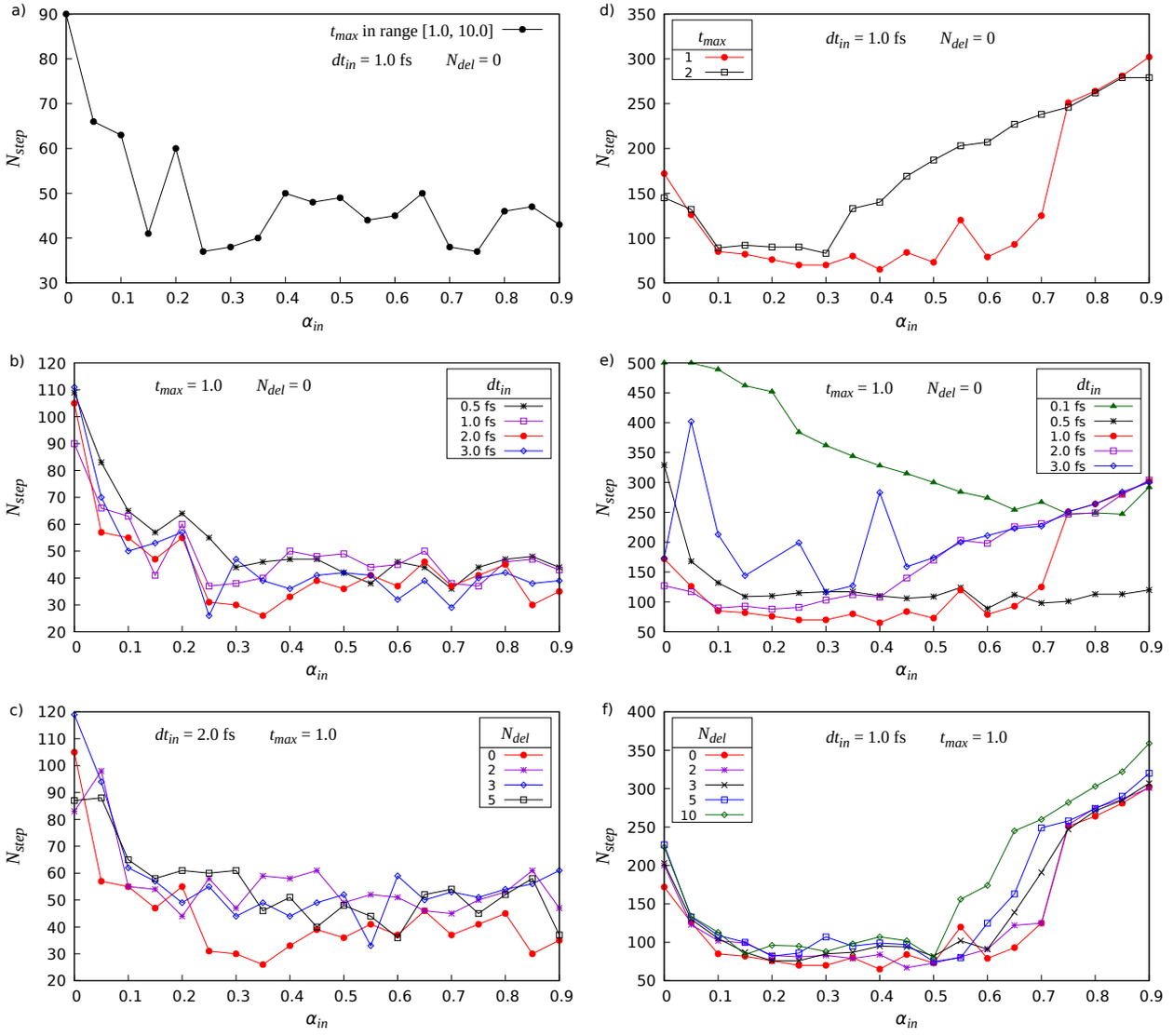

FIG. 1: FIRE parameters $(\alpha_{in}, dt_{in}, t_{max}, N_{del})$ for (left panel: a,b,c) water molecule (0D system, 3 atoms) and (right panel: d,e,f) water polymer (1D system, 6 atoms): screening and setting of the default values.

pretation is confirmed by the average values of the root-mean-square nuclei displacements $\bar{d}_{rms}$ in FIRE optimization, which is roughly one order of magnitude smaller than the correspondent values for quasi-Newton methods SH and BFGS, for almost all the examined atomic systems (see Tables III, IV and Table 13 of the SM). To a minor extent, the better efficiency of a single FIRE step can also be explained by the fact that the updating of nuclei velocities and positions involved in FIRE are very fast operations, while the approximation of the Hessian matrix at each iteration in SH and BFGS methods is slightly more computational expensive, so that the FIRE saving in CPU time increases with the system size. However, since the computational time for the calculation of ground state wavefunction and forces greatly overwhelms the time exploited by all the other remaining operations at each step, the greater efficiency of a single FIRE iteration can be almost entirely ascribed to the reduction of system displacement in the PES at each iteration. At the same time, FIRE takes more iterations to reach convergence, so that its efficiency is comparable with the BFGS one when the increasing in the number of iterations is counterbalanced by the decreasing in the computational cost of each step. Nevertheless, for almost all the systems, FIRE performs better than quasi-Newton SH updating scheme.

As for the reliability of the results, i.e. the capability of finding stationary minima in the PES, the agreement on the final energies and atomic positions between FIRE and BFGS is within the accuracy of the computational set up. The overall root mean square differences between bonds of the structures obtained with FIRE and BFGS, Δb_{rms}, are of the same order of magnitude of the final root mean square displacements, d^{e}_{rms}, suggesting that the optimized geometries

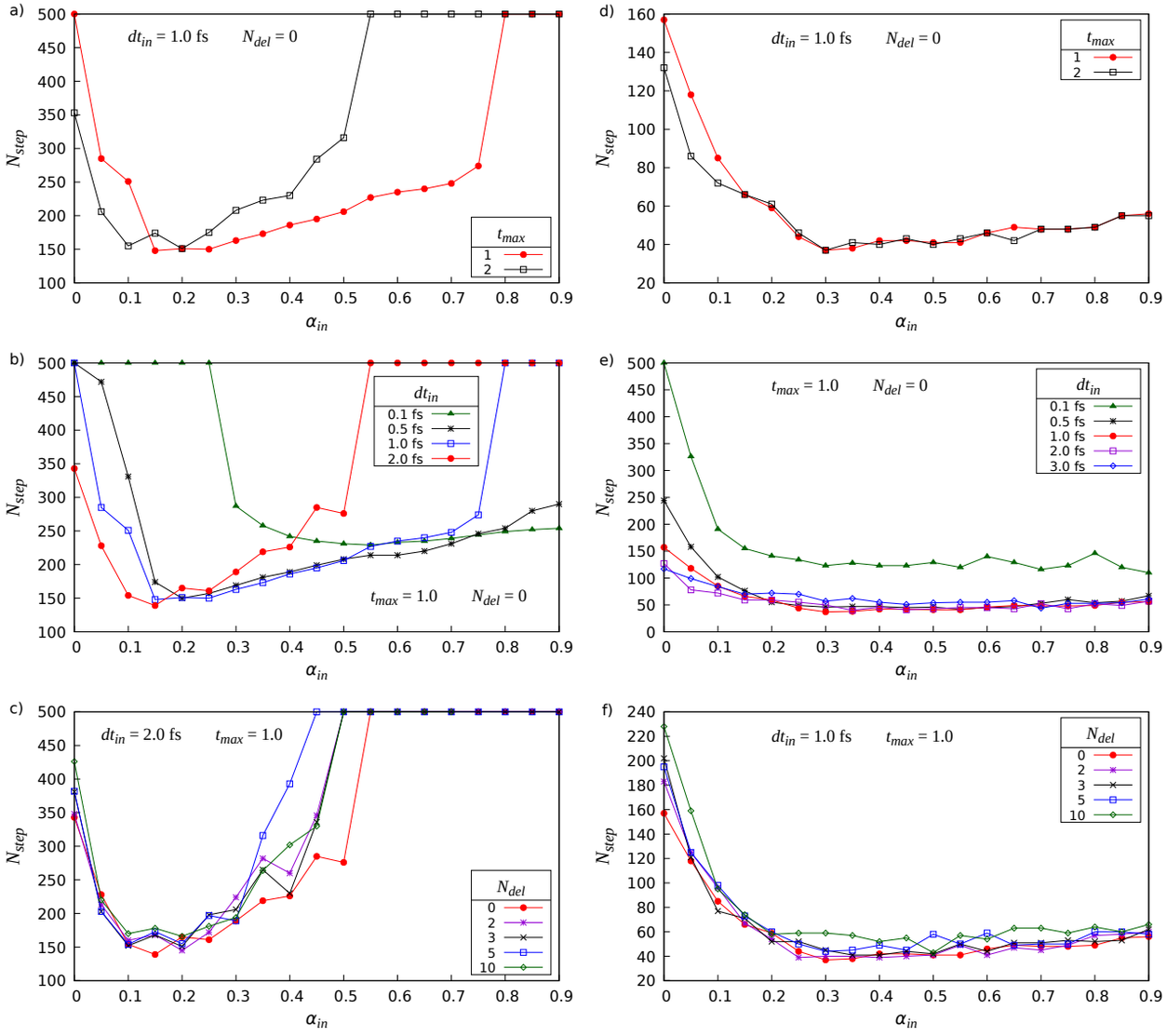

FIG. 2: FIRE parameters ($\alpha_{in}, dt_{in}, t_{max}, N_{del}$) for (left panel: a,b,c) water slab (2D system, 24 atoms) and (right panel: d,e,f) urea molecular crystal (3D system, 16 atoms): screening and setting of the default values.

obtained with the two procedures can be considered equivalent.

Different behaviors in the minimization process were observed and deserve few comments. With reference to the prototypical cases of tempered ice and urea bulk, the mixing factor α, timestep dt, euclidean norm of the $3N$ velocities vector and the power factor are plotted in Fig. 3 as a functions of the number of minimization steps.

In the tempered ice, left panel, after the initial balancing of the system obtained in 10 iterations by efficiently accumulating the inertia, the maximum timestep is reached and both the mixing factor α and the velocities decrease monotonously till convergence. On the contrary, the velocity $\boldsymbol{v}(t)$ of the urea crystal, right panel, brings the trajectory to an uphill motion in the PES several times, so that the timestep is periodically decreased by a factor dt_{dec}, and reaches its maximum value in a nearly stable way only after 27 iterations. A change in the number of equilibration steps, N_{del}, from 0 to 5, does not modify the behavior of α and dt during the minimization of both systems but, within the accuracy on energies and forces, the number of iterations N_{step} increases slightly, passing from 84 to 86 and from 37 to 44, respectively, for tempered ice and urea crystal.

Then, in order to test the robustness and scalability of FIRE and FIRE2.0, given the same set of computational parameters (basis set, DFT functional, FIRE setting as in Table I), structural optimizations of crystalline urea supercells of increasing size were performed. The results, reported in Table III, show that, in the case of FIRE and FIRE2.0 algorithms, the number of iterations does not depend on the system size, so that their efficiency gradually reaches the BFGS one, succeeded in overtaking BFGS computa-

TABLE II: Number of optimization steps N_{step}, average number of wavefunction self-consistent iterations $\bar{N}_w$ required to ground-state convergence, computational time ratio $T_{ratio} = T_{\text{FIRE,SH}}/T_{\text{BFGS}}$, root mean square of final forces $F_{rms} = \|\mathbf{F}\|/\sqrt{3N}$ and of atomic displacements d^e_{rms} in the last cycle, root mean square of bond lengths differences $\Delta b = b_{\text{FIRE,SH}} - b_{\text{BFGS}}$, and energy difference $\Delta E = E_{\text{FIRE}} - E_{\text{BFGS}}$ which results from structural optimizations performed within SH, BFGS and FIRE schemes for different atomic systems with N_{at} atoms. Cartesian coordinates of optimized atomic structures are reported in Figures 10-18 of the Supplementary Material.

System	N_{at}		N_{step}	$\bar{N}_w$	T_{ratio}	F_{rms} [Ha/Bohr]	d^e_{rms} [Bohr]	Δb_{rms} [Bohr]	ΔE [eV/atom]
H_2O (0D)	3	SH	7	6	1.1	$1.76\cdot10^{-7}$	$1.0\cdot10^{-5}$	$1.9\cdot10^{-5}$	$1.0\cdot10^{-12}$
		BFGS	6	6	–	$3.74\cdot10^{-6}$	$4.3\cdot10^{-4}$	–	–
		FIRE	26	5	2.8	$4.31\cdot10^{-7}$	$2.8\cdot10^{-6}$	$1.9\cdot10^{-5}$	$-9.1\cdot10^{-10}$
Water Polymer (1D)	6	SH	26	6	1.3	$1.60\cdot10^{-5}$	$1.0\cdot10^{-3}$	$7.0\cdot10^{-4}$	$1.8\cdot10^{-7}$
		BFGS	21	6	–	$1.32\cdot10^{-5}$	$8.6\cdot10^{-4}$	–	–
		FIRE	65	5	2.6	$5.62\cdot10^{-6}$	$2.4\cdot10^{-5}$	$2.2\cdot10^{-4}$	$3.4\cdot10^{-7}$
Urea (0D)	8	SH	42	8	9.0	$9.04\cdot10^{-5}$	$8.1\cdot10^{-4}$	$1.6\cdot10^{-2}$	$-1.0\cdot10^{-2}$
		BFGS	5	6	–	$1.39\cdot10^{-5}$	$2.8\cdot10^{-4}$	–	–
		FIRE	55	5	8.2	$9.29\cdot10^{-6}$	$9.8\cdot10^{-7}$	$1.0\cdot10^{-4}$	$-4.0\cdot10^{-8}$
Urea (3D)	16	SH	43	7	2.7	$3.13\cdot10^{-6}$	$1.9\cdot10^{-4}$	$5.7\cdot10^{-5}$	$7.8\cdot10^{-7}$
		BFGS	17	6	–	$1.24\cdot10^{-5}$	$4.6\cdot10^{-4}$	–	–
		FIRE	37	5	2.1	$9.85\cdot10^{-6}$	$5.4\cdot10^{-6}$	$5.0\cdot10^{-4}$	$-5.2\cdot10^{-8}$
Water Slab (2D)	24	SH	78	7	2.5	$1.10\cdot10^{-5}$	$5.9\cdot10^{-4}$	$2.5\cdot10^{-4}$	$2.9\cdot10^{-7}$
		BFGS	32	6	–	$1.42\cdot10^{-5}$	$1.1\cdot10^{-3}$	–	–
		FIRE	139	5	4.1	$9.93\cdot10^{-6}$	$4.1\cdot10^{-5}$	$2.2\cdot10^{-4}$	$-5.6\cdot10^{-7}$
Tempered Ice (3D)	24	SH	106	7	2.6	$9.14\cdot10^{-6}$	$4.1\cdot10^{-4}$	$2.6\cdot10^{-4}$	$-7.6\cdot10^{-8}$
		BFGS	41	7	–	$1.12\cdot10^{-5}$	$9.2\cdot10^{-4}$	–	–
		FIRE	84	6	1.9	$9.85\cdot10^{-6}$	$5.2\cdot10^{-4}$	$2.6\cdot10^{-4}$	$-6.7\cdot10^{-6}$
Ice Slab with CO (2D)	32	BFGS	234	8	–	$5.31\cdot10^{-5}$	$5.0\cdot10^{-4}$	–	–
		FIRE	1180	6	4.1	$1.27\cdot10^{-4}$	$8.6\cdot10^{-4}$	$5.3\cdot10^{-3}$	$-2.6\cdot10^{-4}$
Amorphous Ice (3D)	126	BFGS	125	6	–	$2.90\cdot10^{-5}$	$8.1\cdot10^{-4}$	–	–
		FIRE	177	4	1.2	$9.80\cdot10^{-6}$	$1.0\cdot10^{-3}$	$1.4\cdot10^{-2}$	$1.3\cdot10^{-4}$
Crambin (0D)	642	BFGS	530	6	–	$1.18\cdot10^{-5}$	$3.1\cdot10^{-4}$	–	–
		FIRE	530	5	0.8	$8.54\cdot10^{-5}$	$2.1\cdot10^{-3}$	$3.5\cdot10^{-3}$	$6.7\cdot10^{-4}$

tional cost for a number of atoms greater than 192 (3×2×2 supercell). The comparison between FIRE2.0 and the basic FIRE algorithm confirms the higher efficiency of FIRE2.0, which converges to the minimum into a fewer number of optimization steps, retaining at the same time the reliability of the results. Interestingly enough, both the internal accuracy, $\Delta\tilde{E}$, and the agreement with BFGS results, ΔE, are preserved, moving from 16 to 192 atoms (with a corresponding number of atomic orbitals in the basis set equal to 152 and 1824, respectively).

Finally, the dependence of FIRE efficiency on different exchange-correlation functionals, which determine the shape of the PES, was investigated. The influence of the functional on the best setting of FIRE computational parameters (i.e. α_{in}, dt_{in}, t_{max} and N_{del}) was already pointed out in Section III C. Nevertheless, in order to perform a comparison on the same ground, the structural optimization of urea crystal was performed with PBE, B3LYP, HSE06 and PBE0 functionals, adopting the FIRE default values optimized for PBE (see Table I). The results, summarized in Table IV, show that, despite the predictable increase in the computational time due to the non-optimal tuning of the FIRE parameters, the geometries and energies obtained with different functionals are in good agreement with the corresponding BFGS ones, confirming the general portability and robustness of the FIRE optimization procedure. Moreover, the FIRE2.0 algorithms performs better, in terms of number of iterations up to convergence and computational cost, than the basic FIRE, especially for HSE06 and PBE0 hybrid functionals.

V. CONCLUSIONS AND PERSPECTIVES

In this work, we have described the implementation of FIRE algorithm, in its basic and improved (FIRE2.0) versions, and assessed its efficiency and reliability in the CRYSTAL code. FIRE is a structural optimization method based on Molecular Dynamics concepts, intro-

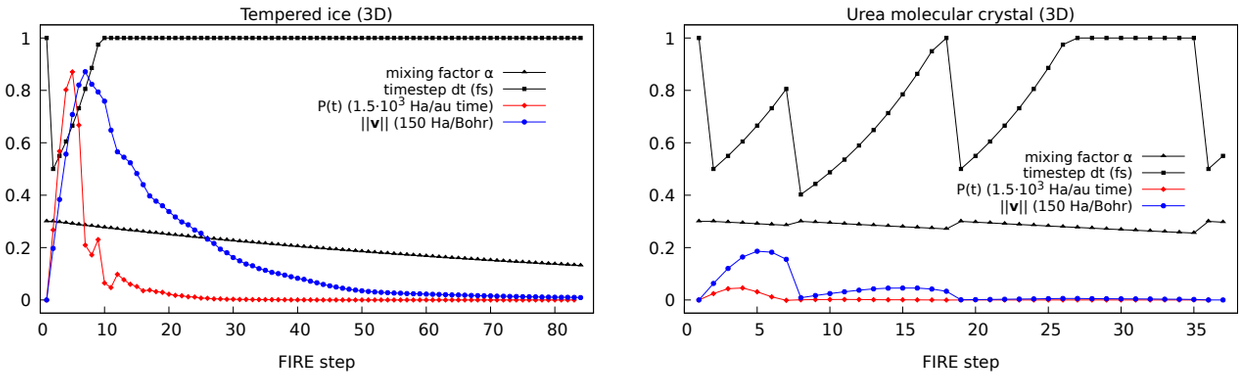

FIG. 3: Behavior of FIRE parameters during the structural optimization of the tempered ice (left panel) and urea molecular crystal (right panel). The values of power factor and of euclidean norm of velocities vector have been amplified by a factor $1.5 \cdot 10^3$ and 150, respectively, to allow comparison with the other parameters.

TABLE III: Number of atoms N_{at} in the supercell, number of atomic orbitals N_{AOs} in the basis set, number of optimization steps N_{step}, average of self-consistent cycles for ground state wavefunction calculation $\bar{N}_w$, ratio of total computational times $T_{ratio} = T_{\text{FIRE}}/T_{\text{BFGS}}$, mean of root-mean-square of atomic displacements $\bar{d}_{rms}$, internal check on energy $\Delta\tilde{E} = E^{16}_{\text{opt}}/16 - E^{N_{at}}_{\text{opt}}/N_{at}$ and final energy difference between the two methods $\Delta E = E_{\text{FIRE}} - E_{\text{BFGS}}$, for different urea molecular crystal (3D) supercell size. The mean values $\bar{N}_w$ and $\bar{d}_{rms}$ are computed by averaging over, respectively, the N_w and d_{rms} values for all the optimization steps. Cartesian coordinates of optimized atomic structures are reported in Figures 19-24 of the Supplementary Material.

Supercell	N_{at}	N_{AOs}		N_{step}	$\bar{N}_w$	T_{ratio}	$\bar{d}_{rms}$ [Bohr]	$\Delta\tilde{E}$ [$\frac{\text{eV}}{\text{atom}}$]	ΔE [$\frac{\text{eV}}{\text{atom}}$]
1×1×1	16	152	BFGS	17	6	–	$1.20 \cdot 10^{-2}$	–	–
			FIRE	37	5	2.11	$1.61 \cdot 10^{-3}$	–	$-5.95 \cdot 10^{-8}$
			FIRE2.0	36	5	1.93	$1.81 \cdot 10^{-3}$	–	$6.86 \cdot 10^{-7}$
2×1×1	32	304	BFGS	21	7	–	$1.56 \cdot 10^{-2}$	$9.42 \cdot 10^{-7}$	–
			FIRE	37	5	1.68	$1.60 \cdot 10^{-3}$	$-2.76 \cdot 10^{-7}$	$1.16 \cdot 10^{-6}$
			FIRE2.0	35	6	1.52	$1.85 \cdot 10^{-3}$	$2.79 \cdot 10^{-7}$	$1.35 \cdot 10^{-6}$
2×2×1	64	608	BFGS	20	8	–	$2.03 \cdot 10^{-2}$	$3.38 \cdot 10^{-6}$	–
			FIRE	37	6	1.59	$1.60 \cdot 10^{-3}$	$-5.21 \cdot 10^{-7}$	$3.84 \cdot 10^{-6}$
			FIRE2.0	35	6	1.47	$1.85 \cdot 10^{-3}$	$7.60 \cdot 10^{-8}$	$3.99 \cdot 10^{-6}$
3×2×1	96	912	BFGS	29	7	–	$9.73 \cdot 10^{-3}$	$1.34 \cdot 10^{-6}$	–
			FIRE	37	6	1.05	$1.61 \cdot 10^{-3}$	$-4.56 \cdot 10^{-7}$	$1.73 \cdot 10^{-6}$
			FIRE2.0	35	6	1.01	$1.85 \cdot 10^{-3}$	$4.59 \cdot 10^{-9}$	$2.02 \cdot 10^{-6}$
2×2×2	128	1216	BFGS	25	8	–	$1.48 \cdot 10^{-2}$	$6.01 \cdot 10^{-6}$	–
			FIRE	37	7	1.11	$1.61 \cdot 10^{-3}$	$1.92 \cdot 10^{-6}$	$4.03 \cdot 10^{-6}$
			FIRE2.0	33	7	1.04	$1.96 \cdot 10^{-3}$	$2.48 \cdot 10^{-6}$	$4.22 \cdot 10^{-6}$
3×2×2	192	1824	BFGS	29	9	–	$1.00 \cdot 10^{-2}$	$3.19 \cdot 10^{-6}$	–
			FIRE	37	7	0.95	$1.61 \cdot 10^{-3}$	$1.90 \cdot 10^{-6}$	$1.23 \cdot 10^{-6}$
			FIRE2.0	33	7	0.90	$1.96 \cdot 10^{-3}$	$2.51 \cdot 10^{-6}$	$1.37 \cdot 10^{-6}$

duced by E. Bitzek et al.[13] as an alternative scheme to quasi-Newton line-search based minimization algorithms. The interest for this novel method is twofold. Firstly, it does not rely on any approximation on the shape of the PES, possibly resulting in good convergence behavior regardless the PES form. Secondly, it does not involve the Hessian approximation, maybe leading to a less computational cost than SH and BFGS schemes.

First of all, a screening of the four FIRE adjustable parameters has been realized through structural optimizations of atomic systems with different dimensionality, identifying a set of robust default values. Then, structural optimizations of atomic systems with different number of atoms, dimensionality and kind of bonds have been performed with FIRE algorithm. The accuracy of FIRE in finding energy minima of the PES for these systems has been demonstrated comparing the total energy and geometry of FIRE final structures with those obtained with quasi-Newton SH and BFGS

TABLE IV: Number of optimization steps N_{step}, average of self-consistent cycles for ground state wavefunction calculation $\bar{N}_w$, computational time ratio $T_{ratio} = T_{\text{FIRE}}/T_{\text{BFGS}}$, mean of root-mean-square of atomic displacements $\bar{d}_{rms}$, final root mean square of nuclear forces $F_{rms} = \|\mathbf{F}\|/\sqrt{3N}$ and of last step atomic displacements d^e_{rms}, and energy difference $\Delta E = E_{\text{FIRE}} - E_{\text{BFGS}}$ which results from structural optimizations of urea crystal (16 atoms) performed with FIRE and BFGS, for different exchange-correlation functionals. Cartesian coordinates of optimized atomic structures are reported in Figures 25-28 of the Supplementary Material.

Functional		N_{step}	$\bar{N}_w$	T_{ratio}	$\bar{d}_{rms}$ [Bohr]	F_{rms} [$\frac{\text{Ha}}{\text{Bohr}}$]	d^e_{rms} [Bohr]	ΔE [$\frac{\text{eV}}{\text{atom}}$]
PBE	BFGS	17	6	–	$1.20 \cdot 10^{-2}$	$1.24 \cdot 10^{-5}$	$4.6 \cdot 10^{-4}$	–
	FIRE	37	5	2.1	$1.61 \cdot 10^{-3}$	$9.85 \cdot 10^{-6}$	$5.4 \cdot 10^{-6}$	$-5.20 \cdot 10^{-8}$
	FIRE2.0	36	5	1.9	$1.81 \cdot 10^{-3}$	$8.47 \cdot 10^{-6}$	$1.3 \cdot 10^{-6}$	$6.95 \cdot 10^{-7}$
B3LYP	BFGS	17	5	–	$3.62 \cdot 10^{-3}$	$2.81 \cdot 10^{-5}$	$3.1 \cdot 10^{-4}$	–
	FIRE	43	4	2.4	$7.15 \cdot 10^{-4}$	$8.54 \cdot 10^{-6}$	$1.5 \cdot 10^{-4}$	$1.56 \cdot 10^{-8}$
	FIRE2.0	43	4	2.4	$7.79 \cdot 10^{-4}$	$9.62 \cdot 10^{-6}$	$1.7 \cdot 10^{-4}$	$-2.64 \cdot 10^{-7}$
HSE06	BFGS	16	5	–	$4.43 \cdot 10^{-3}$	$2.44 \cdot 10^{-5}$	$5.6 \cdot 10^{-4}$	–
	FIRE	58	4	3.4	$4.61 \cdot 10^{-4}$	$9.61 \cdot 10^{-6}$	$1.8 \cdot 10^{-4}$	$1.95 \cdot 10^{-6}$
	FIRE2.0	50	4	3.0	$5.30 \cdot 10^{-4}$	$9.62 \cdot 10^{-6}$	$1.8 \cdot 10^{-4}$	$2.08 \cdot 10^{-6}$
PBE0	BFGS	14	6	–	$4.49 \cdot 10^{-3}$	$2.69 \cdot 10^{-5}$	$4.6 \cdot 10^{-4}$	–
	FIRE	56	4	3.7	$4.60 \cdot 10^{-4}$	$9.73 \cdot 10^{-6}$	$1.4 \cdot 10^{-4}$	$6.34 \cdot 10^{-7}$
	FIRE2.0	48	4	3.2	$5.31 \cdot 10^{-4}$	$9.37 \cdot 10^{-6}$	$1.5 \cdot 10^{-4}$	$9.41 \cdot 10^{-7}$

schemes. The reliability of FIRE and FIRE2.0 in minimize the PES shaped by different functionals, such as PBE, B3LYP, HSE06 and PBE0 has been proven for the case of urea molecular crystal. The FIRE2.0 improved version has proven to be less computational expensive than the basic FIRE one, while maintaining the same accuracy and reliability in finding energy minimum. Finally, as regards the computational time, we can conclude that FIRE and FIRE2.0 structural optimizations have generally a greater computational cost than the correspondent BFGS one, due to the fact that they employ more iterations to reach convergence. Nevertheless, a single FIRE and FIRE2.0 step has a less computational cost than a SH or BFGS one, so that the overall FIRE minimization becomes the most efficient one when the increasing of the computational cost due to a greater number of iterations is compensated for by a reduction of timings in performing each single step.

This study sets the ground for further improvements of a well-structured MD module in the CRYSTAL code. Furthermore, the fact that FIRE algorithm is based on MD concepts could paved the way for other important implementations, namely, a finite temperature structural optimization algorithm and the Nudged Elastic Band method for transition states calculations.

VI. COMPUTATIONAL DETAILS

The new implementation of the FIRE algorithm described in this work has been performed in a beta version of the CRYSTAL package for *ab initio* quantum chemistry and physics of solid state, based on the last public release of the code.[8] The beta version with FIRE structural minimization embedded in can be available for code development or testing purposes by contacting the authors of this article, while a public version of the CRYSTAL program with included the FIRE algorithm will become available in a next public release of the program (conceivably in version CRYSTAL26), that will be obtained through an academic license at a symbolic price for GNU/Linux, MacOSx and Windows operating systems. All the calculations reported in the manuscript are performed with the beta version of the program, based on the CRYSTAL17 public release.[8]

All the atomic systems considered in this article are treated in the frame of the Density Functional Theory (DFT), adopting the gradient-corrected Perdew-Burke-Ernzerhof (PBE) functional,[29] except the crambin molecule that is described through Hartree-Fock (HF) Hamiltonian with three semi-classical corrections (D3, gCP, SRB), which are added to the HF energies (and atomic and cell gradients) within the so called HF3C method.[30–32] Moreover, to better describe the ice slab with CO molecules and the amorphous ice, in conjunction with PBE functional, London-type pairwise empirical correction to the energy for dispersive interactions as proposed by Grimme[33] and as modified for molecular crystals,[34] is considered, in order to include long-range dispersion contributions to the computed *ab initio* total energy and gradients. Furthermore, hybrid functionals such as B3LYP,[35] HSE06[29,36] and PBE0[37] have been used to model the crystalline urea system.

All-electron basis sets, consisting of contracted Gaussian-type atomic orbital functions (A.O.) are used for all the atoms and are reported in the SM.

The DFT exchange-correlation contribution was evaluated by numerical integration over the unit cell vol-

ume, using a pruned grid,[38,39] with a number of radial and angular points reported in Table 2 of the SM for the different analyzed atomic systems.
The diagonalization of the Hamiltonian matrix and the integration over the reciprocal space is carried out using the Monkhorst-Pack mesh,[40] consisting in a grid of $\boldsymbol{k}$-points defined in the Irreducible part of the first Brillouin Zone (IBZ). The Coulomb and exchange series, summed in direct space, are truncated using overlap criteria thresholds. The number of $\boldsymbol{k}$-points in the IBZ, together with the overlap criteria thresholds for Coulomb and exchange series, and the thresholds for the self-consistent field algorithm convergence on the total energy per unit cell, used for the different atomic systems, are reported in Table 2 of the SM.
The tempered ice 3D system has been obtained using a beta version of CRYSTAL Molecular Dynamics module,[12] starting from the initial configuration of crystalline ice and performing a 80 steps (16 fs) NVE MD simulation, with a timestep of 0.2 fs and an initial temperature of 1800 K (the temperature at the 80-th step is equal to 816.5 K).
Geometry optimization is performed using analytical gradients with respect to atomic coordinates, within a quasi-Newtonian algorithm combined with two kinds of Hessian updating schemes: the Schlegel's (SH)[11] and the Broyden-Fletcher-Goldfarb-Shanno (BFGS) formulae.[3–7] Only atomic coordinates are optimized, to allow comparison with FIRE structural minimization. Convergence criteria for SH and BFGS structural optimizations are based on the root mean square and absolute value of the largest component of both the estimated displacements and the gradients of energy functional with respect to the nuclear positions, both computed in normal coordinates. In this framework, the CRYSTAL17 default convergence thresholds and minimization parameters have been adopted.[8,41]

VII. SUPPLEMENTARY MATERIAL

The Supplementary Material (SM) made available contains geometry information about the cell parameters and the atomic coordinates of the structures optimized with both FIRE or FIRE2.0 and BFGS schemes, for each atomic system tested and analyzed in this work. Computational details adopted in the structural optimization calculations are also reported, together with some blocks of the CRYSTAL Input files used for simulations. Further details about average root-mean-square atomic displacements $\bar{d}_{rms}$ in SH, BFGS and FIRE optimizations for the systems considered in Table II are also given in Table 13 of the SM.

VIII. ACKNOWLEDGMENTS

The authors thank Professor Piero Ugliengo for bringing our attention to alternative and novel methods in *ab initio* structural optimization strategies. Thanks also to Professor Alessandro Erba, for useful discussions and hints on algorithm testing methodologies.

IX. DATA AVAILABILITY STATEMENT

The data that supports the findings of this study are available within the article and its Supplementary Material.

X. AUTHOR DECLARATIONS

The authors have no conflicts to disclose.

XI. REFERENCES

[1] J. Nocedal and S. J. Wright, *Numerical Optimization*, 2nd ed. (Springer, New York, USA, 2006).
[2] W. H. Press, B. P. Flannery, S. A. Teukolsky, and W. T. Vetterling, *Numerical Recipes in FORTRAN 77: The Art of Scientific Computing*, 2nd ed. (Cambridge University Press, 1992).
[3] C. G. Broyden, "The convergence of a class of double-rank minimization algorithms 1. General considerations," IMA J. Appl. Math. **6**, 76–90 (1970).
[4] C. G. Broyden, "The convergence of a class of double-rank minimization algorithms 2. The new algorithm," IMA J. Appl. Math. **6**, 222–231 (1970).
[5] R. Fletcher, "A new approach to variable metric algorithms," Comput. J. **13**, 317–322 (1970).
[6] D. Goldfarb, "A family of variable-metric methods derived by variational means," Math. Comput. **24**, 23–26 (1970).
[7] D. Shanno, "Conditioning of quasi-Newton methods for function minimization," Math. Comput. **24**, 647–656 (1970).
[8] R. Dovesi, A. Erba, R. Orlando, C. Zicovich-Wilson, B. Civalleri, L. Maschio, M. Rérat, S. Casassa, J. Baima, S. Salustro, and B. Kirtman, "Quantum-mechanical condensed matter simulations with CRYSTAL," Wiley Interdiscip. Rev. Comput. Mol. Sci. **8**, e1360 (2018).
[9] H. B. Schlegel, "Estimating the hessian for gradient-type geometry optimizations," Theoret. Chim. Acta **66**, 333–340 (1984).
[10] J. M. Wittbrodt and H. B. Schlegel, "Estimating stretching force constants for geometry optimization," J. Mol. Struct. **398-399**, 55–61 (1997).
[11] H. B. Schlegel, "Optimization of equilibrium geometries and transition structures," J. Comput. Chem. **3**, 214–218 (1982).
[12] C. Ribaldone, J. Baima, and S. Casassa, "Implementation of ab initio Born-Oppenheimer Molecular Dynamics in CRYSTAL code," , in preparation (2022).
[13] E. Bitzek, P. Koskinen, F. Gähler, M. Moseler, and P. Gumbsch, "Structural relaxation made simple," Phys. Rev. Lett. **97**, 170201 (2006).
[14] J. Guénolé, W. G. Nöhring, A. Vaid, F. Houllé, Z. Xie, A. Prakash, and E. Bitzek, "Assessment and optimization of the fast inertial relaxation engine (FIRE) for energy minimization in atomistic simulations and its implementation in LAMMPS," Comput. Mater. Sci. **175**, 109584 (2020).
[15] P. Koskinen, S. Malola, and H. Häkkinen, "Self-passivating edge reconstructions of graphene," Phys. Rev. Lett. **101**, 115502 (2008).
[16] J. A. Flores-Livas, A. Sanna, and E. K. Gross, "High temperature superconductivity in sulfur and selenium hydrides at high pressure," Eur. Phys. J. B **89**, 1–7 (2016).
[17] M. Walter and M. Moseler, "Ligand-protected gold alloy clusters: doping the superatom," J. Phys. Chem. C **113**, 15834–15837 (2009).

[18]J. A. Flores-Livas, M. Amsler, T. J. Lenosky, L. Lehtovaara, S. Botti, M. A. L. Marques, and S. Goedecker, "High-pressure structures of disilane and their superconducting properties," Phys. Rev. Lett. **108**, 117004 (2012).
[19]F. Shuang, P. Xiao, R. Shi, F. Ke, and Y. Bai, "Influence of integration formulations on the performance of the fast inertial relaxation engine (FIRE) method," Comput. Mater. Sci. **156**, 135–141 (2019).
[20]D. Sheppard, R. Terrell, and G. Henkelman, "Optimization methods for finding minimum energy paths," J. Chem. Phys. **128**, 134106 (2008).
[21]B. Schaefer, S. Alireza Ghasemi, S. Roy, and S. Goedecker, "Stabilized quasi- Newton optimization of noisy potential energy surfaces," J. Chem. Phys. **142**, 034112 (2015).
[22]S. Plimpton, "Fast parallel algorithms for short-range molecular dynamics," J. Comput. Phys. **117**, 1–19 (1995).
[23]M. J. Abraham, T. Murtola, R. Schulz, S. Páll, J. C. Smith, B. Hess, and E. Lindahl, "GROMACS: high performance molecular simulations through multi-level parallelism from laptops to supercomputers," SoftwareX **1-2**, 19–25 (2015).
[24]J. Stadler, R. Mikulla, and H. Trebin, "IMD: a software package for molecular dynamics studies on parallel computers," Int. J. Mod. Phys. C **08**, 1131–1140 (1997).
[25]W. Smith, C. Yong, and P. Rodger, "DL_POLY: application to molecular simulation," Mol. Simul. **28**, 385–471 (2002).
[26]S. Chill, M. Welborn, R. Terrell, L. Zhang, J. Berthet, A. Pedersen, H. Jónsson, and G. Henkelman, "EON: software for long time simulations of atomic scale systems," Model. Simul. Mat. Sci. Eng. **22**, 055002 (2014).
[27]A. H. Larsen, J. J. Mortensen, J. Blomqvist, I. E. Castelli, R. Christensen, M. Dulak, J. Friis, M. Groves, B. Hammer, C. Hargus, E. D. Hermes, P. C. Jennings, P. B. Jensen, J. Kermode, J. Kitchin, E. L. Kolsbjerg, J. Kubal, K. Kaasbjerg, S. Lysgaard, J. B. Maronsson, T. Maxson, T. Olsen, L. Pastewka, A. A. Peterson, C. Rostgaard, J. Schiøtz, O. Schütt, M. Strange, K. Thygesen, T. Vegge, L. Vilhelmsen, M. Walter, Z. Zeng, and K. W. Jacobsen, "The atomic simulation environment-a python library for working with atoms," J. Phys. Condens. Matter **29**, 273002 (2017).
[28]R. P. Feynman, "Forces in molecules," Phys. Rev. **56**, 340–343 (1939).
[29]J. P. Perdew, K. Burke, and M. Ernzerhof, "Generalized gradient approximation made simple," Phys. Rev. Lett. **77**, 3865–3868 (1996).
[30]R. Sure and S. Grimme, "Corrected small basis set Hartree-Fock method for large systems," J. Comput. Chem. **34**, 1672–1685 (2013).
[31]J. Brandenburg and S. Grimme, "Dispersion corrected Hartree-Fock and density functional theory for organic crystal structure prediction," Top. Curr. Chem. **345**, 1–23 (2013).
[32]M. Cutini, B. Civalleri, M. Corno, R. Orlando, J. Brandenburg, L. Maschio, and P. Ugliengo, "Assessment of different quantum mechanical methods for the prediction of structure and cohesive energy of molecular crystals," J. Chem. Theory Comput. **12**, 3340–3352 (2016).
[33]S. Grimme, "Semiempirical GGA-type density functional constructed with a long-range dispersion correction," J. Comput. Chem. **27**, 1787–1799 (2006).
[34]B. Civalleri, C. M. Zicovich-Wilson, L. Valenzano, and P. Ugliengo, "B3LYP augmented with an empirical dispersion term (B3LYP-D*) as applied to molecular crystals," CrystEngComm **10**, 405–410 (2008).
[35]A. D. Becke, "Density functional thermochemistry. III. The role of exact exchange," J. Chem. Phys. **98**, 5648–5652 (1993).
[36]A. V. Krukau, O. A. Vydrov, A. F. Izmaylov, and G. E. Scuseria, "Influence of the exchange screening parameter on the performance of screened hybrid functionals," J. Chem. Phys. **125**, 224106 (2006).
[37]C. Adamo and V. Barone, "Toward reliable density functional methods without adjustable parameters: the PBE0 model," J. Chem. Phys. **110**, 6158–6170 (1999).
[38]A. D. Becke, "A multicenter numerical integration scheme for polyatomic molecules," J. Chem. Phys. **88**, 2547–2553 (1988).
[39]M. D. Towler, A. Zupan, and M. Causà, "Density functional theory in periodic systems using local gaussian basis sets," Comput. Phys. Commun. **98**, 181–205 (1996).
[40]H. J. Monkhorst and J. D. Pack, "Special points for Brillouin-zone integrations," Phys. Rev. B **13**, 5188–5192 (1976).
[41]R. Dovesi, V. R. Saunders, C. Roetti, R. Orlando, C. M. Zicovich-Wilson, F. Pascale, B. Civalleri, K. Doll, N. M. Harrison, I. J. Bush, P. D'Arco, M. Llunel, M. Causà, Y. Noel, L. Maschio, A. Erba, M. Rérat, and S. Casassa, "CRYSTAL17 User's Manual," https://www.crystal.unito.it/manuals/crystal17.pdf , (2018).

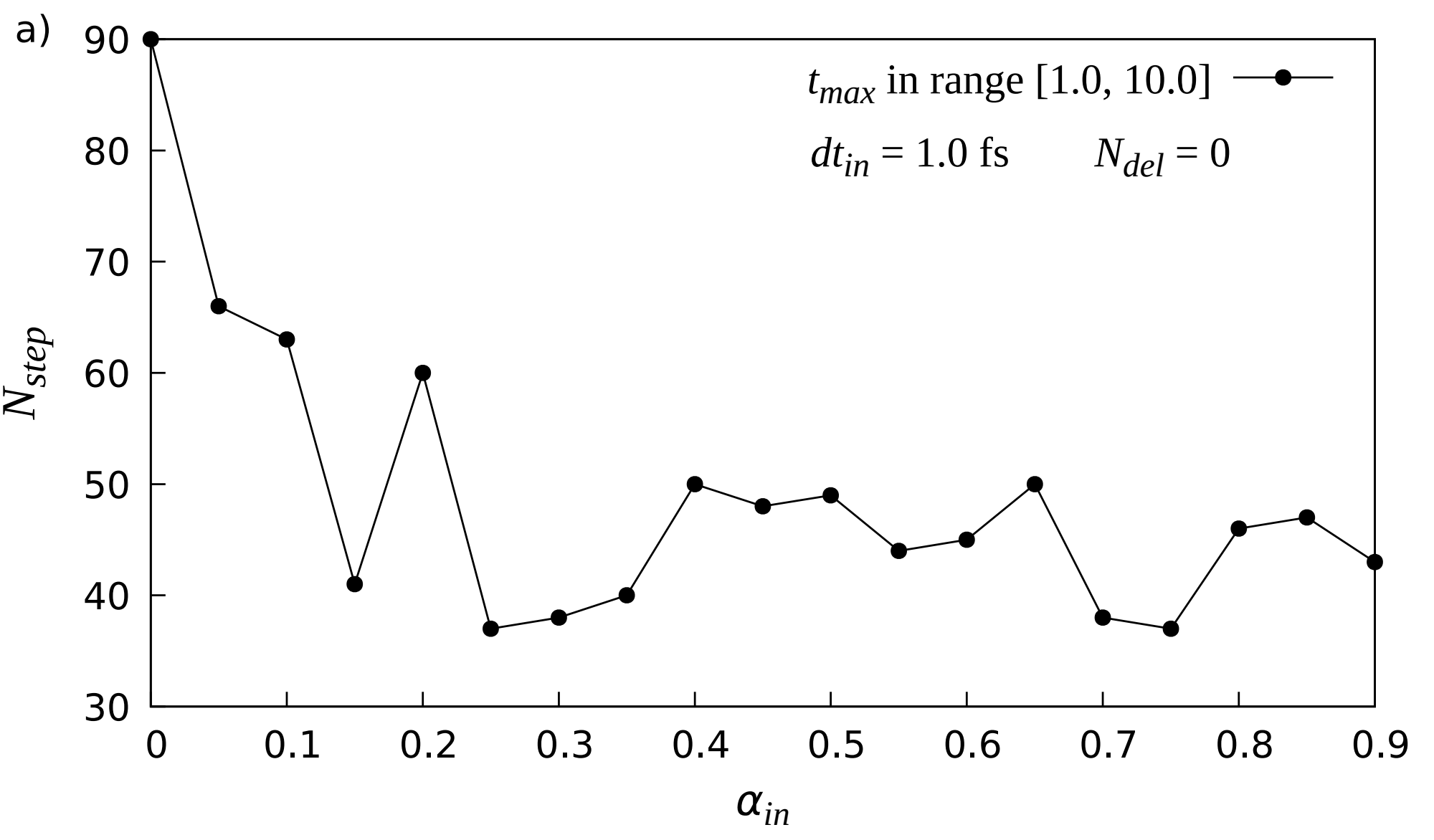
a)
t_{max} in range [1.0, 10.0]
dt_{in} = 1.0 fs
N_{del} = 0
N_{step}
α_{in}
90
80
70
60
50
40
30
0
0.1
0.2
0.3
0.4
0.5
0.6
0.7
0.8
0.9

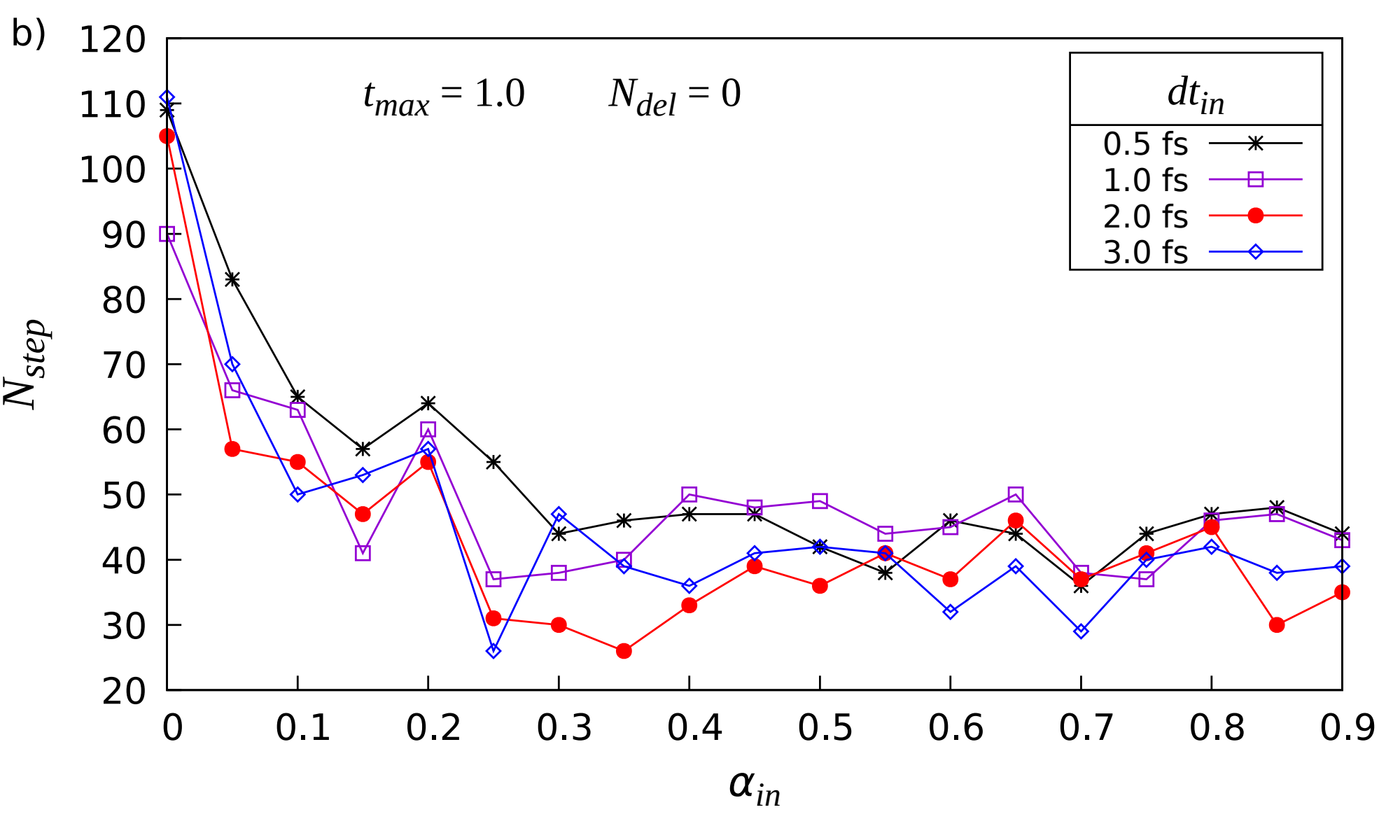
b)
t_{max} = 1.0
N_{del} = 0
dt_{in}
0.5 fs
1.0 fs
2.0 fs
3.0 fs
N_{step}
α_{in}
120
110
100
90
80
70
60
50
40
30
20
0
0.1
0.2
0.3
0.4
0.5
0.6
0.7
0.8
0.9

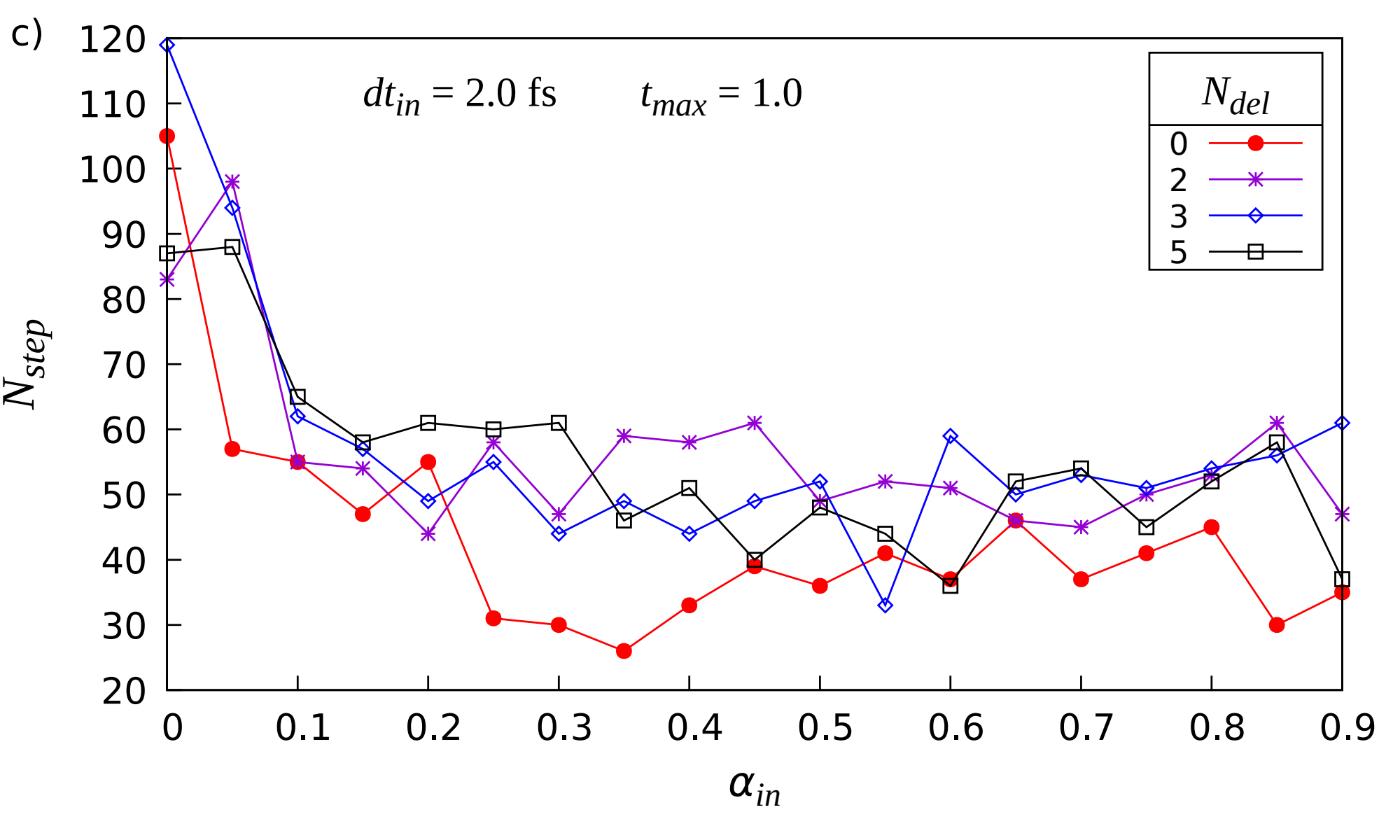
c)
dt_{in} = 2.0 fs
t_{max} = 1.0
N_{del}
0
2
3
5
N_{step}
α_{in}
120
110
100
90
80
70
60
50
40
30
20
0
0.1
0.2
0.3
0.4
0.5
0.6
0.7
0.8
0.9

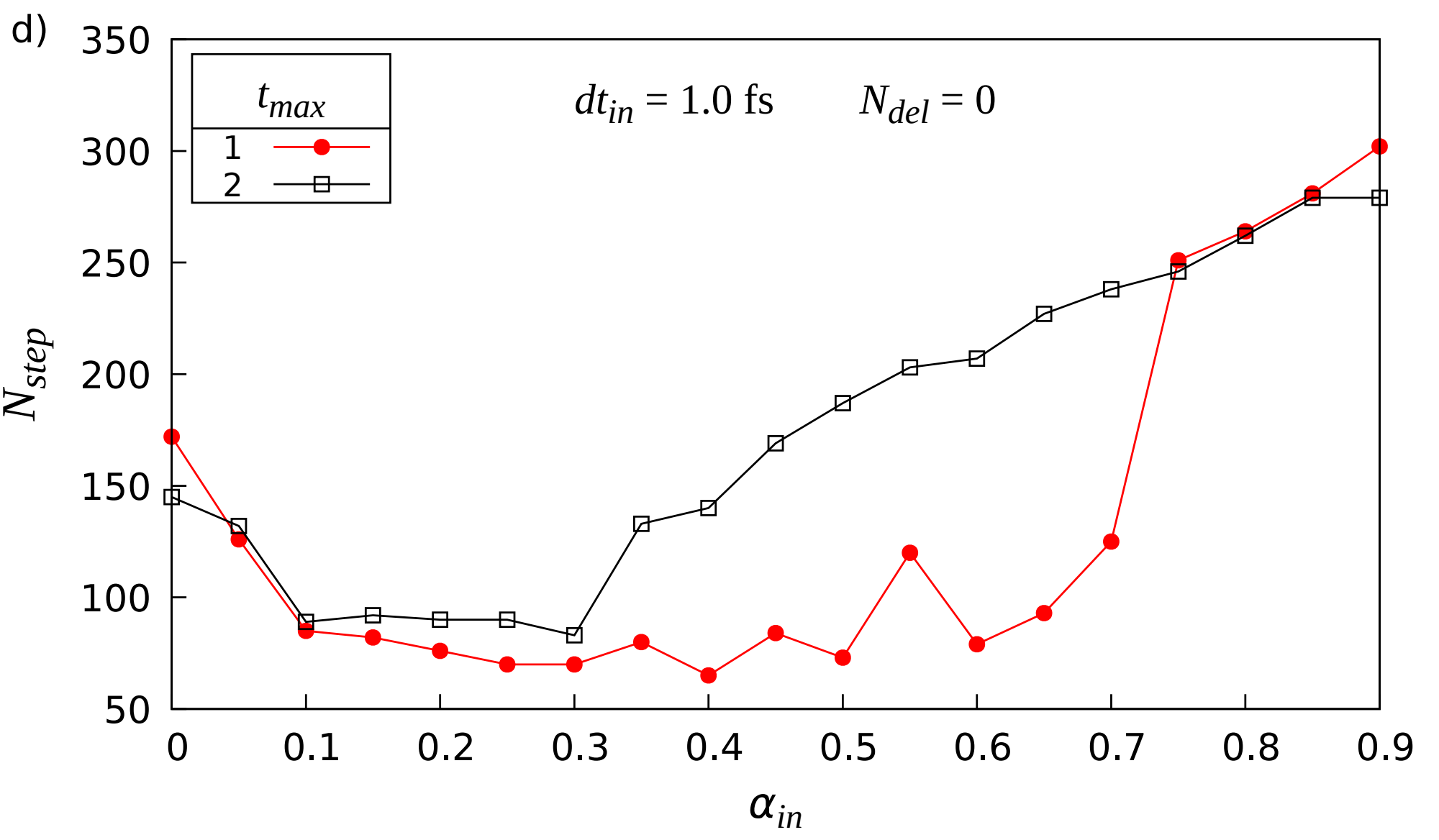
d)
t_{max}
1
2
dt_{in} = 1.0 fs
N_{del} = 0
N_{step}
α_{in}
350
300
250
200
150
100
50
0
0.1
0.2
0.3
0.4
0.5
0.6
0.7
0.8
0.9

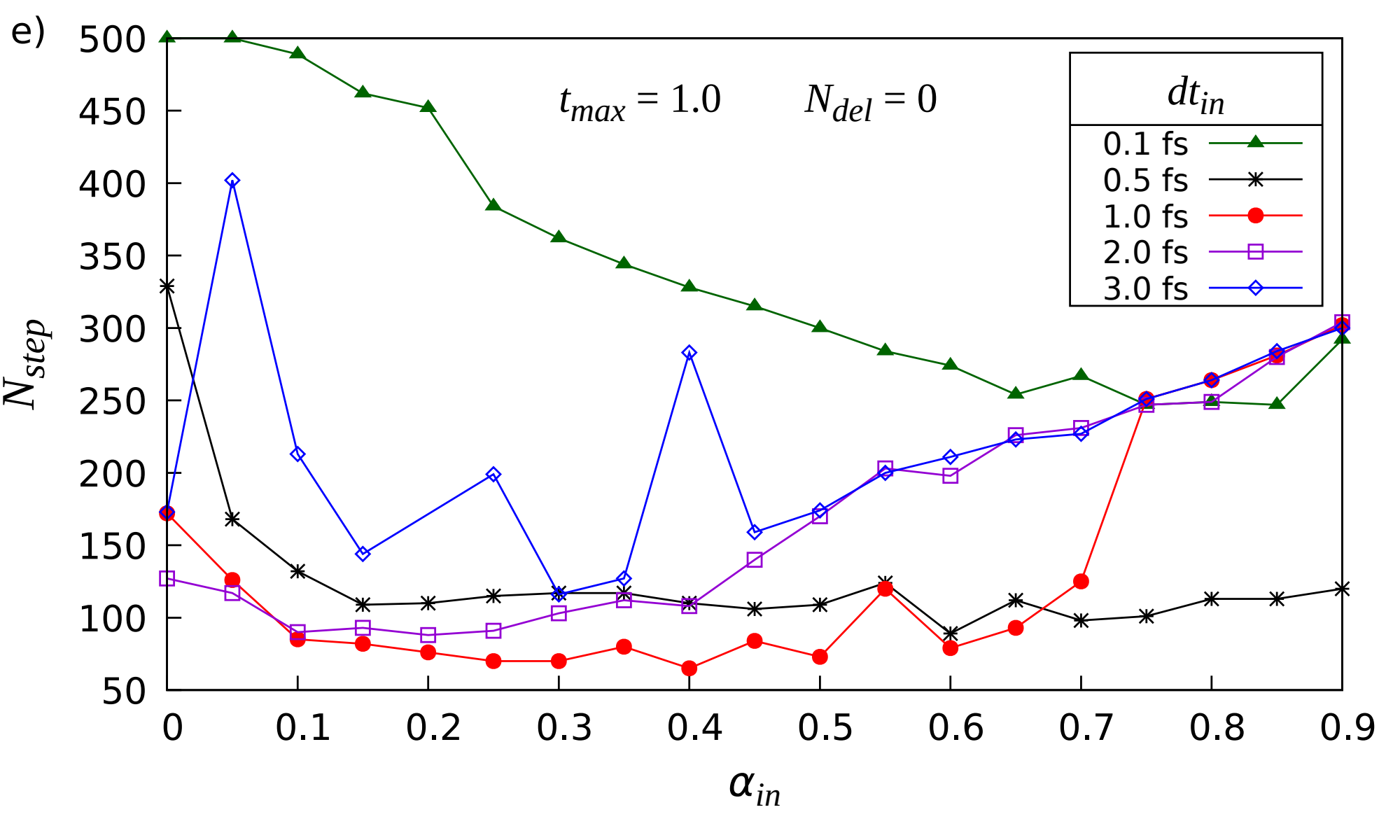
e)
t_{max} = 1.0
N_{del} = 0
dt_{in}
0.1 fs
0.5 fs
1.0 fs
2.0 fs
3.0 fs
N_{step}
α_{in}
500
450
400
350
300
250
200
150
100
50
0
0.1
0.2
0.3
0.4
0.5
0.6
0.7
0.8
0.9

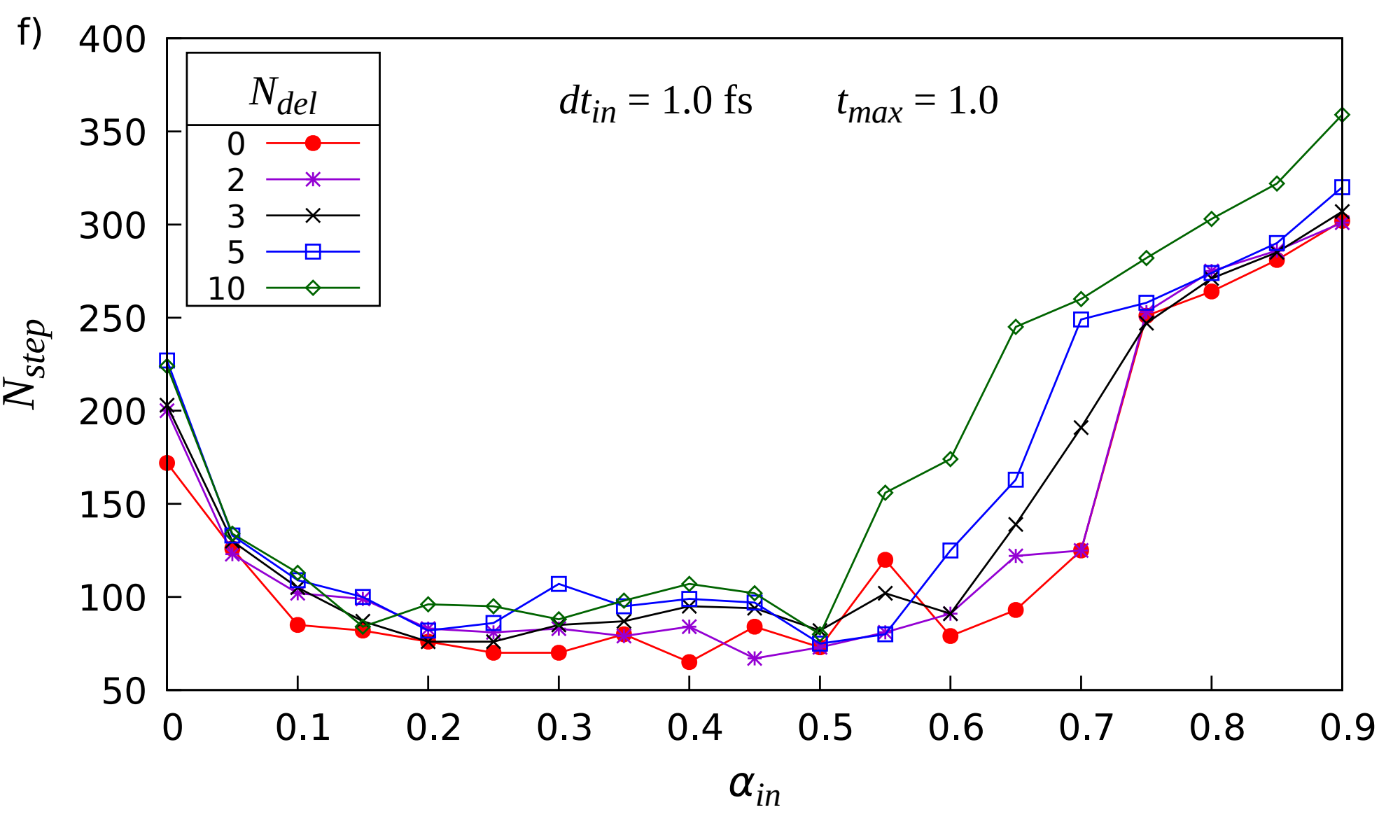
f)
N_{del}
0
2
3
5
10
dt_{in} = 1.0 fs
t_{max} = 1.0
N_{step}
α_{in}
400
350
300
250
200
150
100
50
0
0.1
0.2
0.3
0.4
0.5
0.6
0.7
0.8
0.9

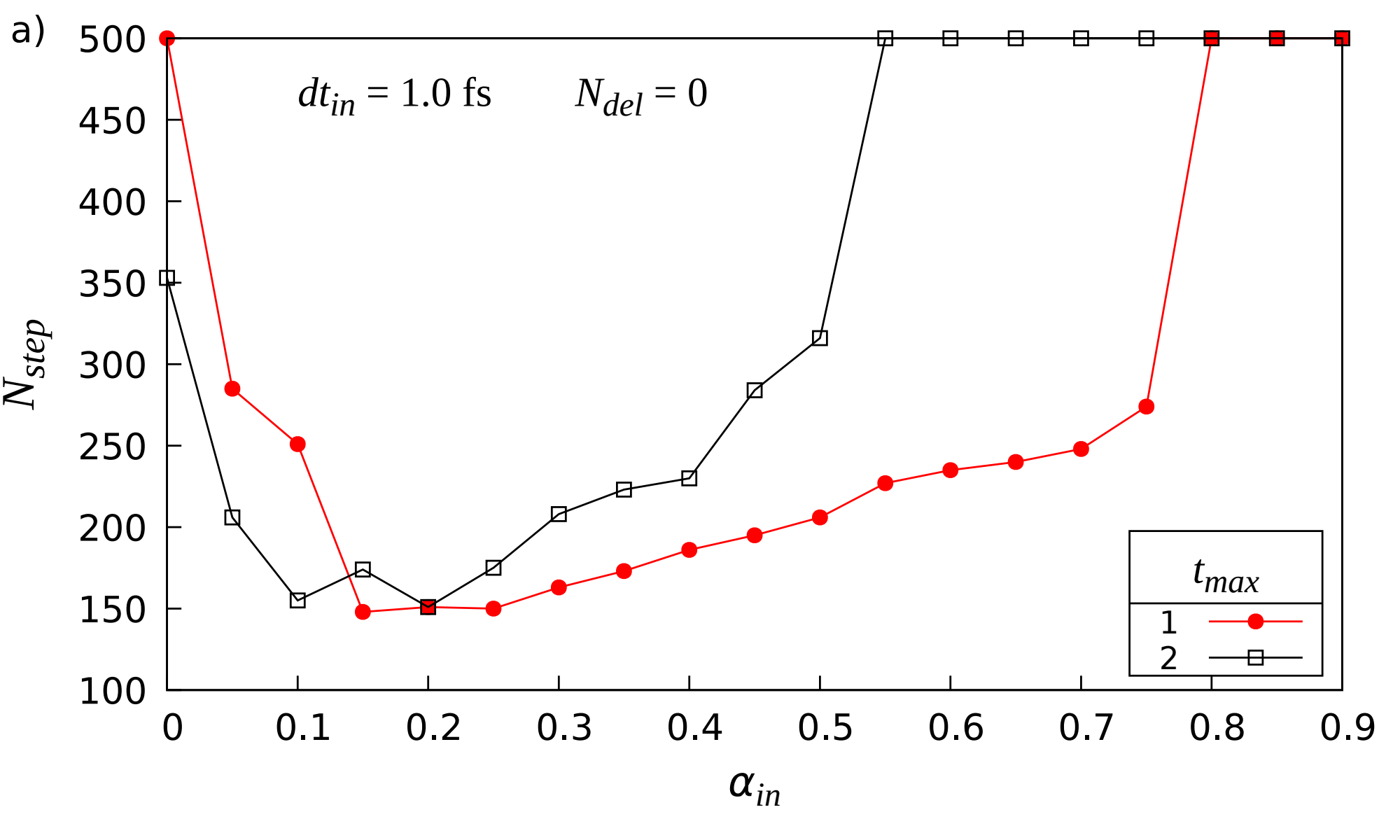
a)
dt_{in} = 1.0 fs
N_{del} = 0
N_{step}
α_{in}
500
450
400
350
300
250
200
150
100
0
0.1
0.2
0.3
0.4
0.5
0.6
0.7
0.8
0.9
t_{max}
1
2

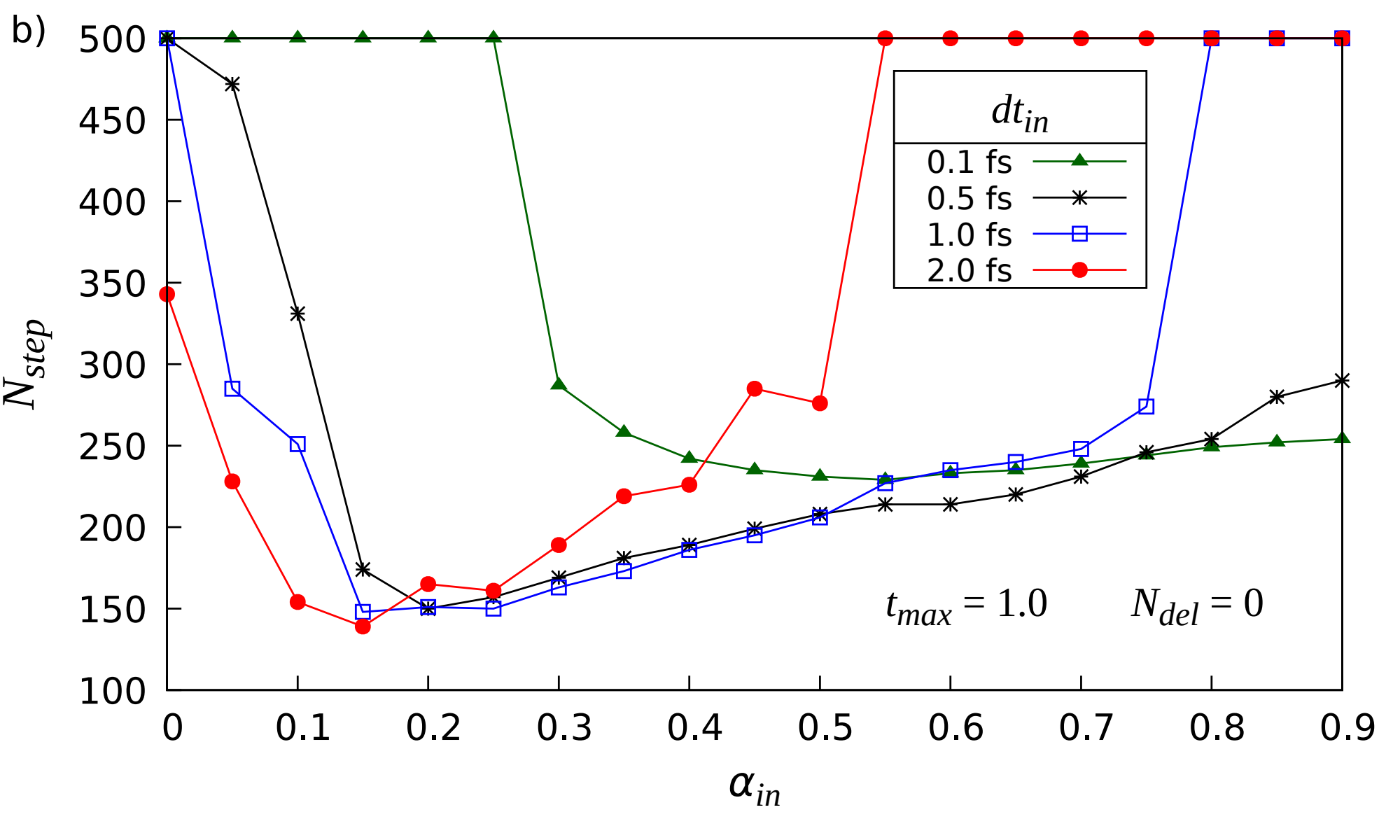
b)
500
450
400
350
300
250
200
150
100
N_{step}
0
0.1
0.2
0.3
0.4
0.5
0.6
0.7
0.8
0.9
α_{in}
dt_{in}
0.1 fs
0.5 fs
1.0 fs
2.0 fs
$t_{max} = 1.0$
$N_{del} = 0$

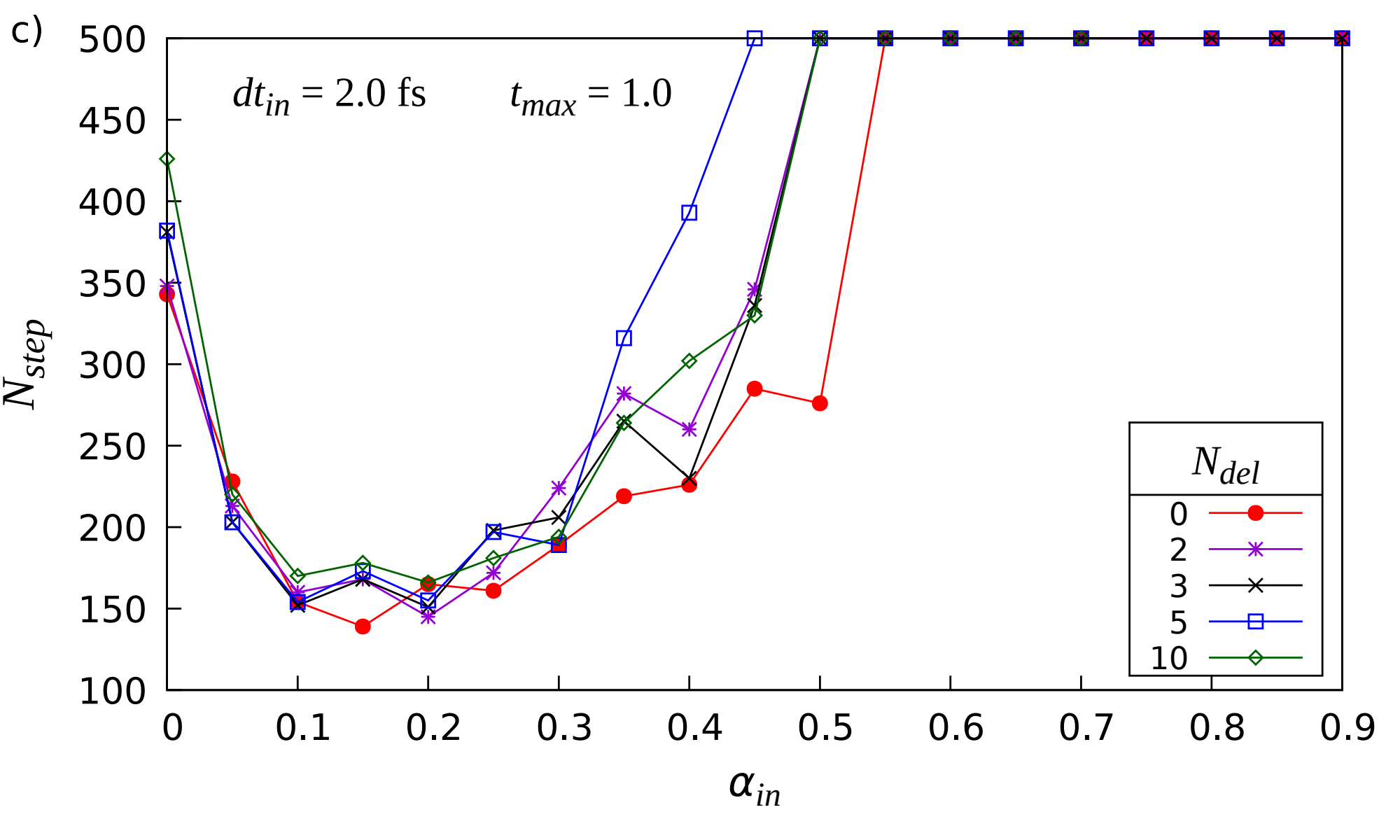
c)
dt_{in} = 2.0 fs
t_{max} = 1.0
N_{step}
α_{in}
N_{del}
0
2
3
5
10
500
450
400
350
300
250
200
150
100
0
0.1
0.2
0.3
0.4
0.5
0.6
0.7
0.8
0.9

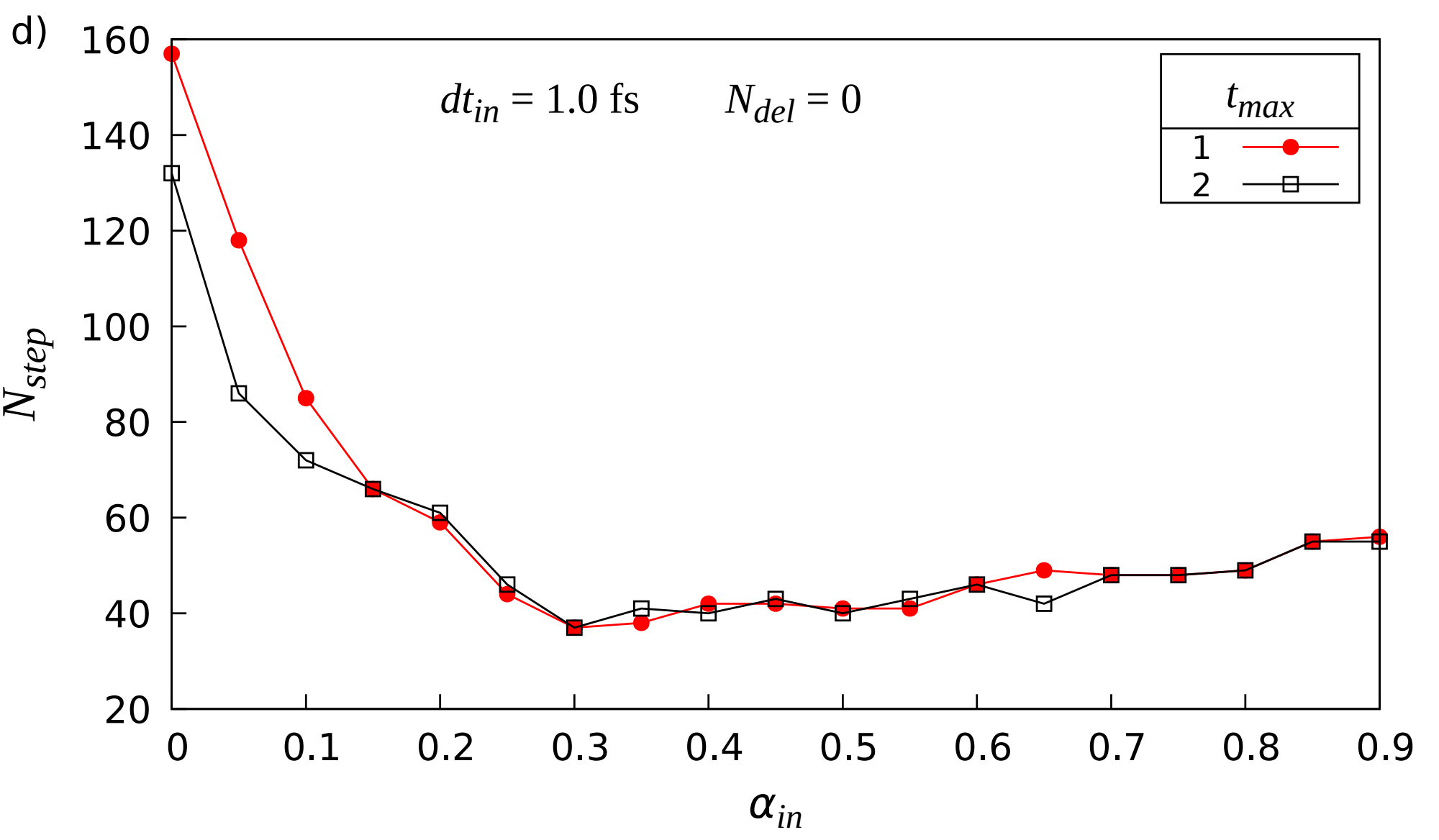
d)
dt_{in} = 1.0 fs
N_{del} = 0
t_{max}
1
2
N_{step}
α_{in}
160
140
120
100
80
60
40
20
0
0.1
0.2
0.3
0.4
0.5
0.6
0.7
0.8
0.9

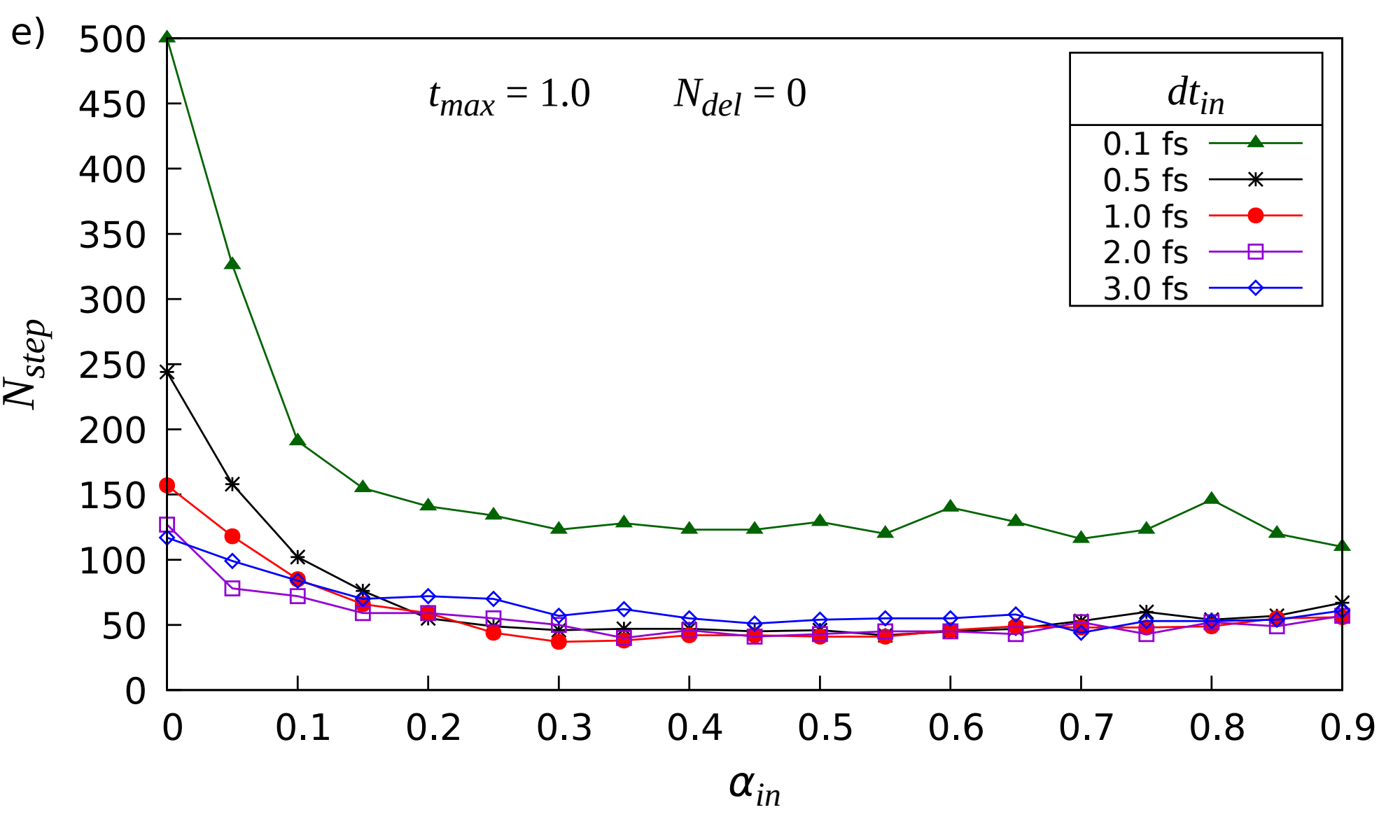
e)
t_{max} = 1.0
N_{del} = 0
dt_{in}
0.1 fs
0.5 fs
1.0 fs
2.0 fs
3.0 fs
N_{step}
α_{in}
0
50
100
150
200
250
300
350
400
450
500
0
0.1
0.2
0.3
0.4
0.5
0.6
0.7
0.8
0.9

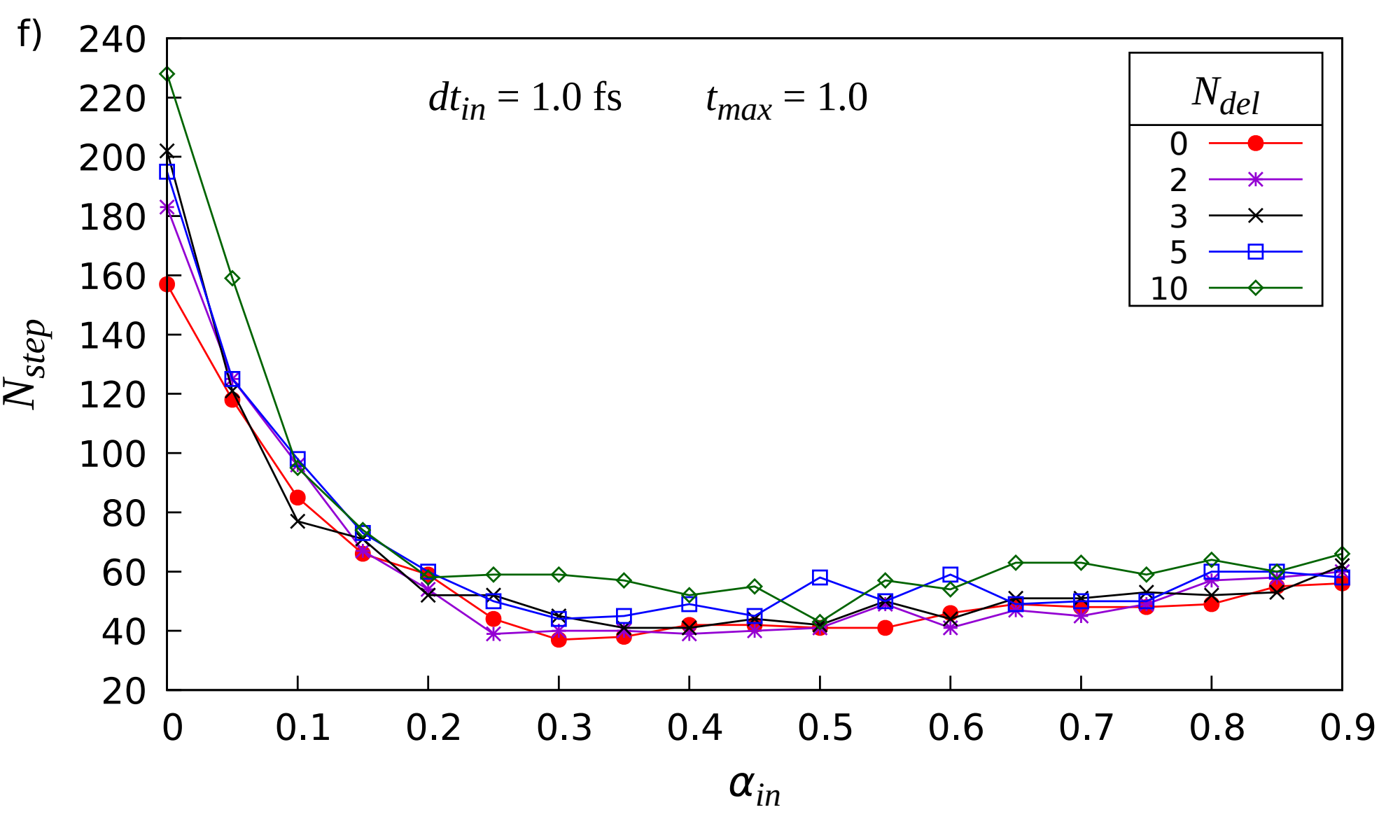
f)
dt_{in} = 1.0 fs
t_{max} = 1.0
N_{del}
0
2
3
5
10
N_{step}
240
220
200
180
160
140
120
100
80
60
40
20
0
0.1
0.2
0.3
0.4
0.5
0.6
0.7
0.8
0.9
α_{in}

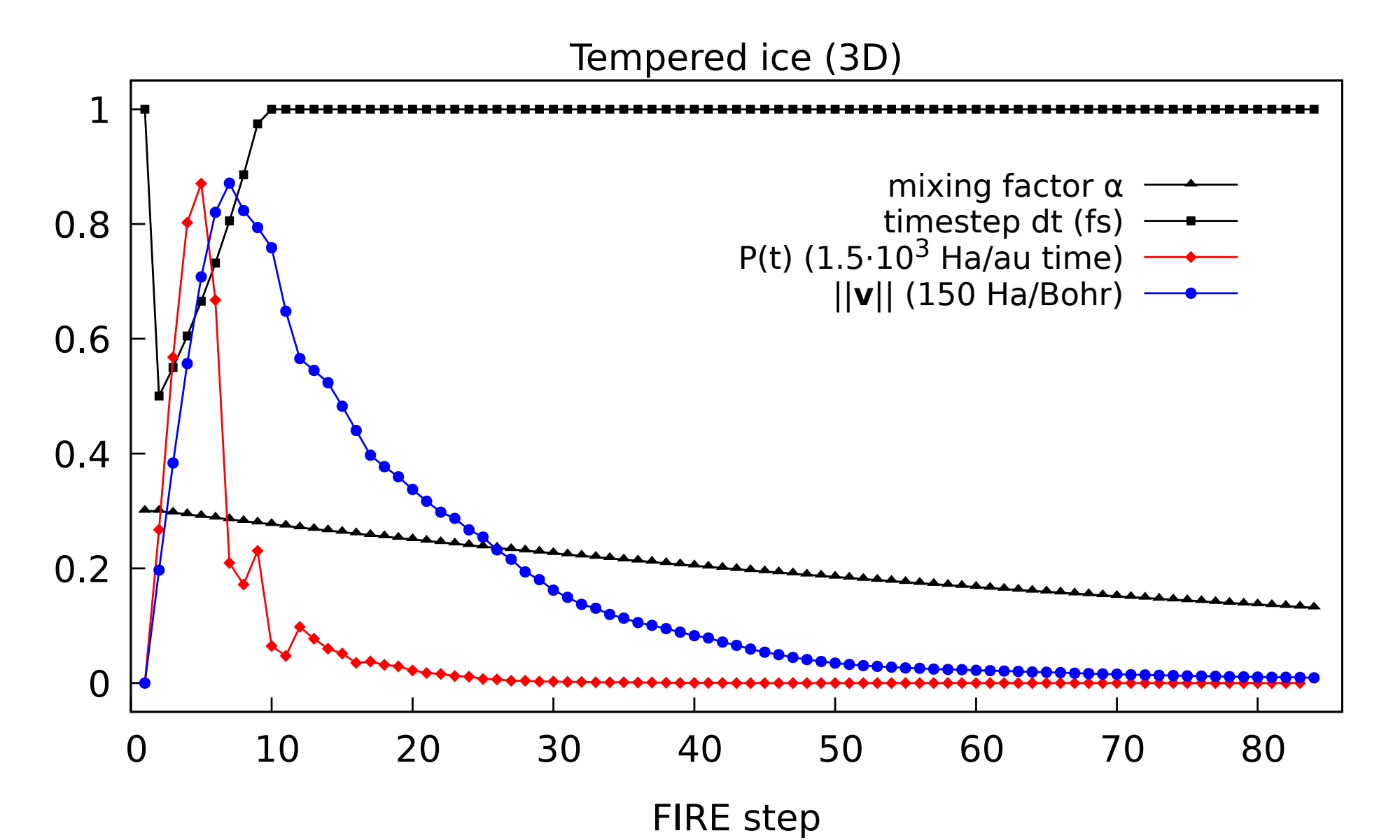
Tempered ice (3D)
mixing factor α
timestep dt (fs)
P(t) (1.5·10^3 Ha/au time)
||v|| (150 Ha/Bohr)
1
0.8
0.6
0.4
0.2
0
0
10
20
30
40
50
60
70
80
FIRE step

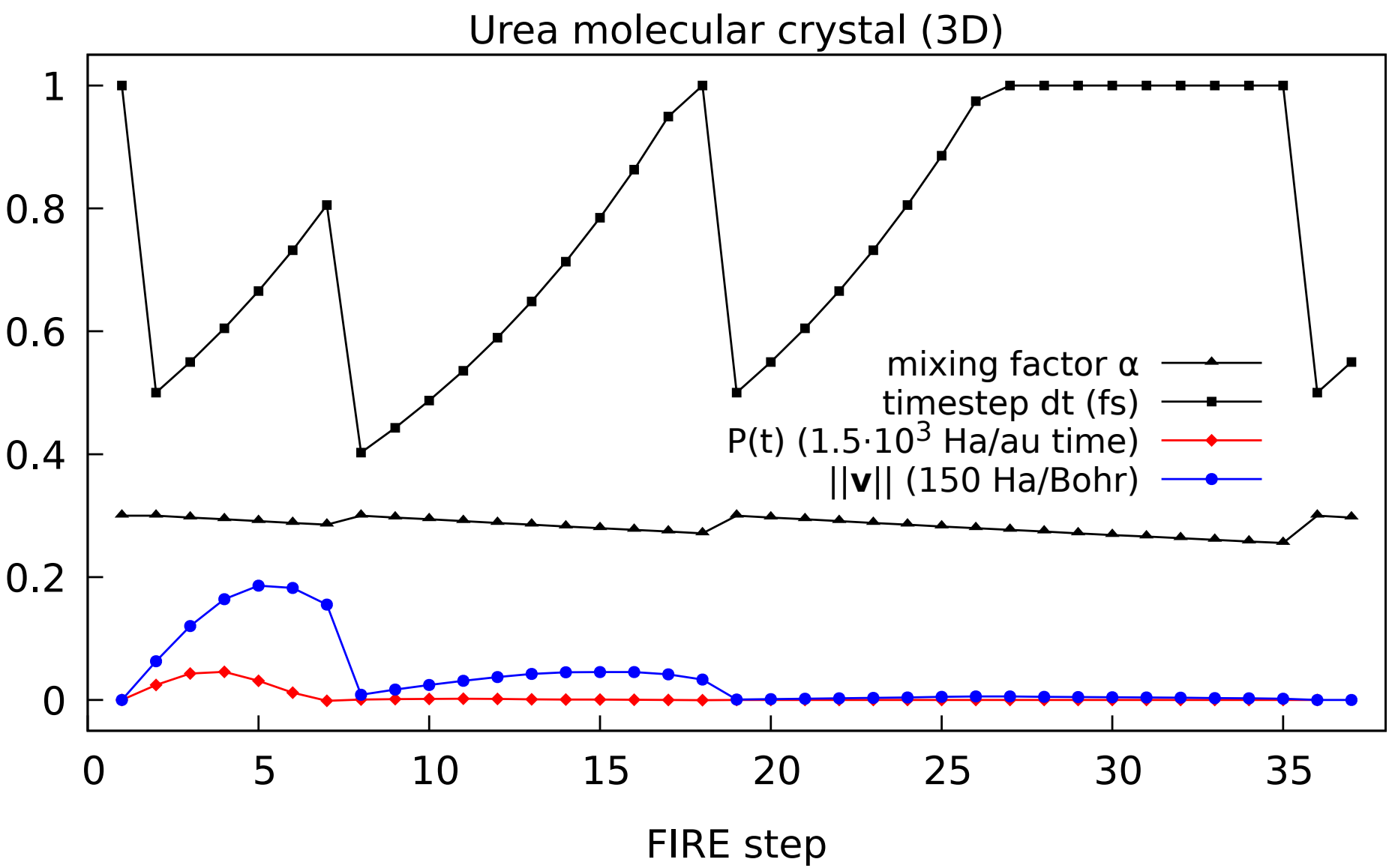
Urea molecular crystal (3D)
1
0.8
0.6
0.4
0.2
0
0
5
10
15
20
25
30
35
FIRE step
mixing factor α
timestep dt (fs)
P(t) (1.5·10^3 Ha/au time)
||v|| (150 Ha/Bohr)